10

Imaging the Lithosphere and Upper Mantle: Where We Are At and Where We Are Going

Juan Carlos Afonso,[1] Max Moorkamp,[2] and Javier Fullea[3,4]

"…It will become clear that the simplicity of the inner Earth is only apparent; with the progress of [experimental and observational] techniques, we may perhaps expect that someday "physics of the interior of the Earth" will make as little sense as "physics of the crust"…"

J.-P. Poirier (1991, *Introduction to the Physics of the Earth's Interior*)

ABSTRACT

Hypotheses and conclusions concerning the physical state of the interior of the Earth are under constant debate. At least part of the controversy lies in the fact that traditionally studies of different nature (i.e., seismic, geochemical, electromagnetic, etc.), with very different spatial and temporal resolutions and sensitivities to the thermochemical structure of the Earth's interior, have been used in isolation to explain the same phenomena (e.g., temperature or velocity anomalies, magmatism, plate motion, strain partitioning, etc.). There is no a priori reason, however, why the results from these diverse studies should be strictly comparable, consistent, or compatible, despite sampling the same physical structure. In recent years, however, advances on computational power, inversion methods, and laboratory experimental techniques, as well as the dramatic increase on both quality and quantity of multiple geophysical and geochemical datasets, have created great interest on integrated (joint) multidisciplinary analyses capable of exploiting the complementary benefits of different datasets/methods. This chapter endeavors to provide a comprehensive review of the current state of the art in such integrated studies of the lithosphere and sublithospheric upper mantle, as well as of their benefits and limitations. Although important stand-alone (single-data) methods are briefly discussed, the emphasis is on forward, inverse, and probabilistic techniques that integrate two or more datasets into a formal joint analysis. The role of emerging trends for imaging the Earth's interior and their potential for elucidating the physical state of the planet are also discussed.

[1]*CCFS—Department of Earth and Planetary Sciences, Macquarie University, Sydney, New South Wales, Australia*

[2]*Department of Geology, University of Leicester, Leicester, United Kingdom*

[3]*Institute of Geosciences (CSIC, UCM), Madrid, Spain*

[4]*Dublin Institute for Advanced Studies, Dublin, Ireland*

10.1. INTRODUCTION

Most information on the physical state of the Earth's interior comes from the application of imperfect geophysical and geochemical theories to sparse observations made at the Earth's surface. Such theories must be

Integrated Imaging of the Earth: Theory and Applications, Geophysical Monograph 218, First Edition.
Edited by Max Moorkamp, Peter G. Lelièvre, Niklas Linde, and Amir Khan.

constantly refined to accommodate an ever-increasing amount of data arriving in the form of field observations and laboratory experiments. At least in part, the substantial increase in the quality and quantity of available datasets and processing power over the past few decades has been responsible for major changes in how we perceive and conceptualize the nature of the Earth's interior. For instance, the advent and development of global tomography has clearly demonstrated that the Earth's upper mantle, once thought to be relatively homogeneous, is highly heterogeneous at various length scales. Comprehensive studies involving large compilations of mantle samples (e.g., xenoliths, ophiolites, abyssal peridotites, etc.) and mantle-derived volcanic rocks provide further support for a complex thermochemical structure of the upper mantle and lithosphere. As a result, it is now widely accepted that the lithospheric and sublithospheric upper mantle are complex physicochemical systems that interact via mass and energy transfer processes over various length and time scales and that these interactions largely control the evolution of important tectonic and geological phenomena. The detection of these interactions and the imaging of the thermochemical structure of the Earth's interior, however, is far from straightforward and currently represent two of the most important and challenging goals of modern geophysics.

In this chapter, we will discuss some of the most relevant methods that are currently used to image the physical state of the lithosphere and upper mantle. While some single-data approaches will be mentioned due to their significant contribution to our understanding of the Earth's interior, we will focus on joint approaches that integrate complementary datasets. Due to length limitations, we cannot hope to include all relevant references in one chapter. We apologize to those authors whose work could not be directly cited.

10.2. GENERAL CONSIDERATIONS ABOUT THE LITHOSPHERE

The Earth's lithosphere consists of the entire crust (oceanic and continental) and a portion of the uppermost upper mantle. It is critical to humans, as most tectonic and biological activities on which modern society depends take place either within or at the boundaries of lithospheric plates. Examples are volcanic and seismic activity, mineralization events, and water and CO_2 recycling, among others. Although many definitions of lithosphere have been proposed in the literature (see Table 10.1), all of them can ultimately be related to the thermochemical state (i.e., temperature, stress field and composition) of the actual rocks making up the crust and uppermost mantle. This stems from the simple fact that important rock properties such as elastic moduli, electrical conductivity, strength, and viscosity are largely controlled by temperature, pressure, lithology (i.e., composition), and H_2O content (cf. *Ranalli* [1995] and *Karato* [2008]). Although rock fabric can in principle affect the strength of the lithosphere, the relative effect of fabric is of second-order compared to that of temperature and/or H_2O content. Therefore, most of the confusion around the use and meaning of different definitions of lithosphere is, in most cases, only apparent. Several review monographs have recently addressed the question of how to best define the lithosphere and the so-called lithosphere–asthenosphere boundary (LAB), as well as the relation between different definitions (e.g., see *Eaton et al*. [2009], *Artemieva* [2009, 2011], and *Kind et al*. [2012]). We emphasize,

Table 10.1 Commonly Used Definitions of "Lithosphere"[a].

Definition	Main Distinctive Feature
Mechanical	Outer part of the Earth where there are no significant vertical gradients in horizontal strain rate (i.e., no internal deformation) and effectively isolated from the underlying convective mantle over geological time scales (cf. *Burov* [2011] and *Turcotte and Schubert* [2014])
Seismological (LID)	High-velocity material that overlies the upper mantle Low Velocity Zone (LVZ) (cf. *Anderson* [1989] and *Fisher et al*. [2010])
Thermal	Material above a critical isotherm where heat is transferred primarily by conduction (cf. *Turcotte and Schubert* [2014] and *Artemieva* [2011])
Elastic	Strong outer shell of the Earth that can support applied loads elastically and without permanent deformation (cf. *Watts* [2001])
Electrical	Outer, generally resistive, layer of the Earth overlying more conductive material (cf. *Jones* [1999] and *Jones and Craven* [2004])
Geochemical	Material that preserve distinct geochemical and isotopic signatures for longer periods than the underlying convecting mantle (cf. *Griffin et al*. [1999] and *O'Reilly and Griffin* [2010])
Petrological	Uppermost portion of the upper mantle where amphibole (magnesian pargasite) is stable (cf. *Green and Fallon* [1998] and *Green et al*. [2010])

[a] We note that different authors assign slightly different characteristics to some of these definitions.

however, that within the plate tectonics paradigm, there is only one strict definition, namely the mechanical or rheological definition (e.g., see *Isacks et al*. [1968] and *Le Pichon et al*. [1973]). Thus, the lithosphere represents the Earth's rigid/strong/viscous outermost shell, which can sustain and transmit relatively large stresses over geologic time scales. It forms relatively rigid plates that move over a hotter and rheologically weaker layer (the asthenosphere) that is characterized by pervasive ductile deformation (solid-state creep) and multiscale convection. Although its formal definition is therefore clear, the impossibility of directly probing the lithospheric mantle gives rise to a number of indirect "technique-based" definitions (Table 10.1).

Given the strong dependence of rock strength on temperature, the so-called "thermal definition" of the lithosphere has some practical and conceptual advantages over other proposed definitions. Being a thermal boundary layer itself, the lithosphere is a nonconvecting region of relatively high temperature gradient (controlled by conduction of heat) between its lower boundary and the Earth's surface. This represents a well-established and important tenant of lithospheric modeling that allows practical estimations of "thermal" lithospheric structures provided appropriate boundary conditions and physical parameters are chosen (cf. *Jaupart and Mareschal* [2011], *Hasterok and Chapman* [2011], *Artemieva* [2011], and *Furlong and Chapman* [2013]). Importantly, through the use of temperature-dependent rheological laws appropriate for lithospheric rocks, a formal relation between the thermal and mechanical definitions can be defined (cf. *Ranalli* [1995], *Kohlstedt et al*. [1995], *Burov* [2011], and *Turcotte and Schubert* [2014]). On the downside, the viscosity of rocks is dependent not only on temperature, but also on pressure, composition, melt content, fluid content, strain rate, and so on (e.g., *Ranalli* [1995], *Kohlstedt and Zimmerman* [1996], *Mei and Kohlstedt* [2000a,b], *Karato* [2008], and *Tasaka et al*. [2013]), and some important parameters such as the activation volumes and energies of the aggregate are still subject to large uncertainties. Thus, a single temperature would not correspond to a single viscosity value everywhere. Whereas the pressure effect is negligible when considering actual uncertainties in temperature estimations from geophysical and/or thermobarometric methods, volatile content, on the other hand, can significantly complicate the relation between temperature and viscosity (cf. *Hirth and Kohlstedt* [1996], *Karato and Jung* [1998], *Mei and Kohlstedt* [2000a,b], *Karato* [2008], and *Burov* [2011]). Also, episodic magmatism and or fluid circulation can locally and temporarily alter conductive geotherms [*Furlong and Chapman*, 2013]. However, significant departures (of the order of 150–250°C at scales of 50–100 km) from a conductive profile are only important in regions that experienced extended tectonothermal events (rifting, orogenesis, subduction) less than ~80 Ma ago [*Furlong and Chapman*, 2013]. With these caveats in mind, the thermal definition of the lithosphere has the advantages of (a) being a practical and reliable working definition, (b) having a formal relation to the mechanical definition, (c) having a direct connection with other popular definitions (e.g., electrical, seismic, etc.) through laboratory-based equations of state for mineral properties (e.g., elastic moduli, electrical conductivity, etc.), and (d) eliminating ambiguities associated with other methods which struggle to locate the LAB beneath some tectonic settings, such as Archean cratons (i.e., the thermal definition always outputs a specific isotherm that can be related to the LAB). All other definitions of lithosphere (Table 10.1) respond to *specific features* related to (but not strictly defining) the nature and evolution of the lithosphere and typically predict significantly different lithospheric thicknesses (e.g., see *Eaton et al*. [2009] and *Jones et al*. [2010]). For instance, the so-called *seismic lithosphere* or lid, is characterized by a layer of relatively high velocities and/or frozen anisotropy (cf. *Anderson* [1989] and *Plomerova et al*. [2002]). These specific features are a consequence, rather than the cause, of the cold and viscous nature of lithospheric rocks compared to the underlying mantle. Likewise, the distinct geochemical signatures used to define a *chemical lithosphere* (e.g., see *Griffin et al*. [1999]) can only exist due to the highly viscous, nonconvecting nature (i.e., thus, no homogenization) of lithospheric rocks.

One of main advantages of adopting the seismic definition of the lithosphere is that one can use global seismic models to estimate the structure of the lithosphere (e.g., *Priestley and McKenzie* [2006], *Conrad and Lithgow-Bertelloni* [2006], *Thybo* [2006], *Lebedev and van der Hilst* [2008], *Fischer et al*. [2013], and *Artemieva* [2011]). *Pasyanos et al*. [2014] have recently applied this principle to construct a 1° tessellated global model of the lithosphere (LITHO1.0) by inverting Love and Rayleigh (group and phase) dispersion data over a wide period range (up to 200 sec). Similarly, *Priestley and McKenzie* [2006] and *Priestley and Tilmann* [2009] also inverted dispersion data to obtain the seismic velocity structure of the upper mantle, which is subsequently used to estimate geotherms and the base of the lithosphere. Despite some minor differences in the data and approach used, these models, as many others before, reveal a great variability in lithospheric thicknesses (either seismological or thermal) worldwide, with a marked long-wavelength correlation between lithospheric thickness and surface tectonics. This correlation has been highlighted before in numerous studies (e.g., *Jordan* [1988], *Anderson* [1989], *Grand* [1994], *Nolet et al*. [1994], and *Zhang and Tanimoto* [1991]) and it represents a robust seismological feature of the upper

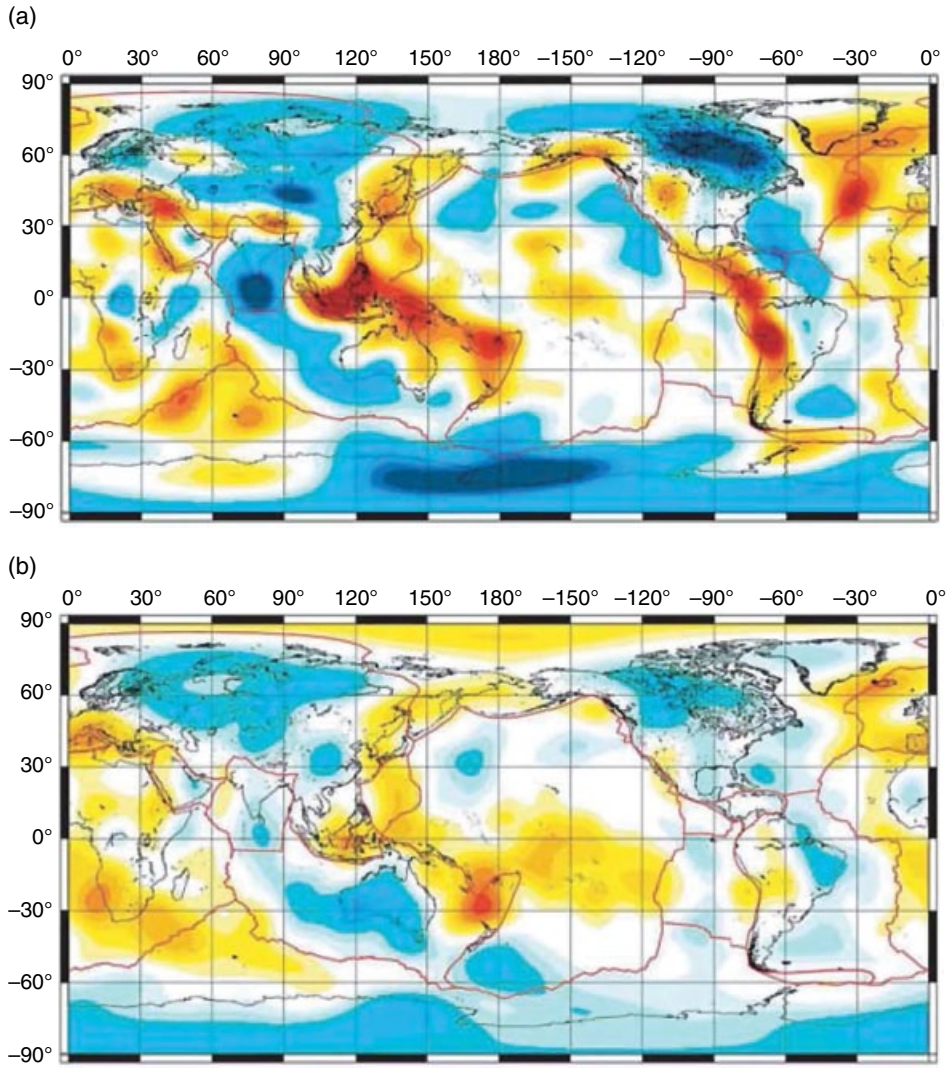

Figure 10.1 **(a)** Observed EGM96 global free-air gravity anomalies. **(b)** The "mean" free-air gravity anomalies derived from global seismic models (mean of five different seismic models). Both observed and predicted anomalies shown are synthesized from spherical harmonics up to degree and order 20. Modified from *Forte* [2007].

mantle. A difficulty with such studies, however, is that when velocity anomalies are converted into density anomalies, the gravity anomalies, induced mantle flow, topography, and plate velocities predicted by the model tend to be poor representations of the real observations (Figure 10.1; *Forte* [2007, 2000] and *Simmons et al*. [2010]). This is not surprising, since the magnitude of the temperature anomalies necessary to significantly affect geodynamic observables is of the same order as the uncertainties associated with temperatures derived from global seismic models. Approaches that include the simultaneous inversion of potential fields and/or geodynamic observables offer an attractive solution (e.g., see *Simmons et al*. [2010]).

Although the base of the lithosphere is commonly thought of as a first-order boundary or structural discontinuity, there are no strong a priori physical arguments why it should be a global sharp boundary. Factors that can contribute to produce a relatively sharp boundary at the base of the lithosphere include the presence of melt lenses, sharp change in fluid content (mainly H_2O), and strong shearing due to the horizontal motion of the plate, among others. Some or all of these factors are likely to be more common in oceanic environments (e.g., *Afonso et al*. [2008b], *Karato* [2012], *Kawakatsu et al*. [2009], *Rychert and Shearer* [2011], *Olugboji et al*. [2013], and *Naif et al*. [2013]), where evidence for sharp seismic discontinuities (which in *some* cases *may* coincide with the

base of the lithosphere) is clear (e.g., *Kawakatsu et al*. [2009] and *Olugboji et al*. [2013]). However, geochemical, geophysical, and numerical evidence suggest that, at least beneath some continents, this boundary is more like a gradual "transitional zone" and subject to complex multi-scale physicochemical interactions between the overlying lithospheric plate and the sublithospheric upper mantle. Some of these interactions include the episodic transfer of mass and energy from the asthenosphere to the base of the lithosphere (e.g., percolation of low-degree melts, refertilization, underplating) and from the lithosphere to the asthenosphere (e.g., lithospheric downwellings or drips, small-scale convection), which can significantly modify the properties of this complex region both in space and time. The term lithosphere–asthenosphere boundary, or LAB, therefore seems to be a bit of a misnomer, especially when used to define lithospheric structure. Perhaps it would more appropriate to simply use lithospheric thickness when referring to lithospheric structure and lithosphere–asthenosphere transition zone (LATZ) or lithosphere–asthenosphere system (LAS) when referring to the complex transitional region between the lithosphere and sublithospheric upper mantle.

10.3. COMPOSITION OF THE UPPER MANTLE

It is commonly agreed that the bulk composition of the upper mantle can be represented as that of a peridotite *sensu lato*. Although this model has been regularly challenged (cf. *Anderson* [1989]), abundant evidence collected in the past 30 years from experimental phase equilibria, mineral physics studies, seismological observations, composition of mantle-derived magmas, and studies of exhumed mantle support a bulk peridotitic upper mantle (cf. *McDonough and Sun* [1995], *Pearson et al*. [2003], and *Bodinier and Godard* [2003]). The four main mineral phases are olivine, clinopyroxene, orthopyroxene, and an aluminum-rich phase. The latter can be either garnet, spinel, or plagioclase, depending on the equilibration pressure (some of these phases can coexist at certain PT conditions). The dominant Al-rich phase present in the rock typically defines the "facies" from which the samples have been recovered (e.g., garnet versus spinel facies). According to the IUGS classification nomenclature, the term "peridotite" is restricted to ultramafic rocks with more than 40% modal olivine (Figure 10.2). Peridotites are further subdivided into lherzolites (abundant amounts of clino- and orthopyroxene), harzburgites (mostly orthopyroxene), dunites (>90% olivine), and wherlites (mostly clinopyroxene), with the first three making up over 90% of all recovered mantle samples (see below). Secondary phases, such as apatite (phosphate), rutile (TiO2), zircon (ZrSiO4), monazite (phosphate), phlogopite (Mg-rich mica), and amphiboles (hydrous silicate), may also be present, especially around localized veins where metasomatizing fluids/melts percolated through mantle rocks [*Pearson et al*., 2003; *O'Reilly and Griffin*, 2013]. Moreover, solidified melts within the lithospheric mantle coupled with fluid–rock interaction processes can result in local, but significant, lithological contrasts (e.g., eclogite and/or pyroxenite bodies; SiO_2-enriched harzburgitic domains, etc. [*Kelemen et al*., 1998; *Jacob*, 2004; *Pearson et al*., 2003; *Bodinier et al*., 2008]). The actual spatial distribution and abundance of ultramafic rocks other than peridotites within the upper mantle is debated and

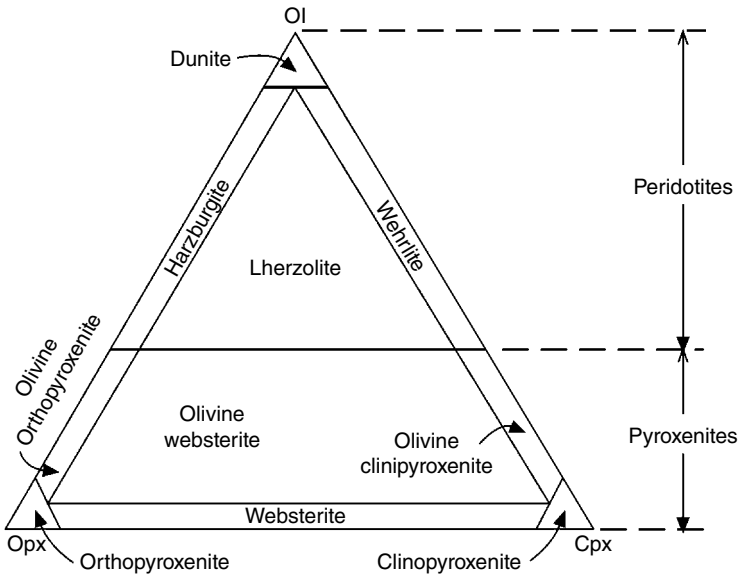

Figure 10.2 IUGS modal classification of major rock types in the lithospheric mantle. After *Streckeisen* [1979].

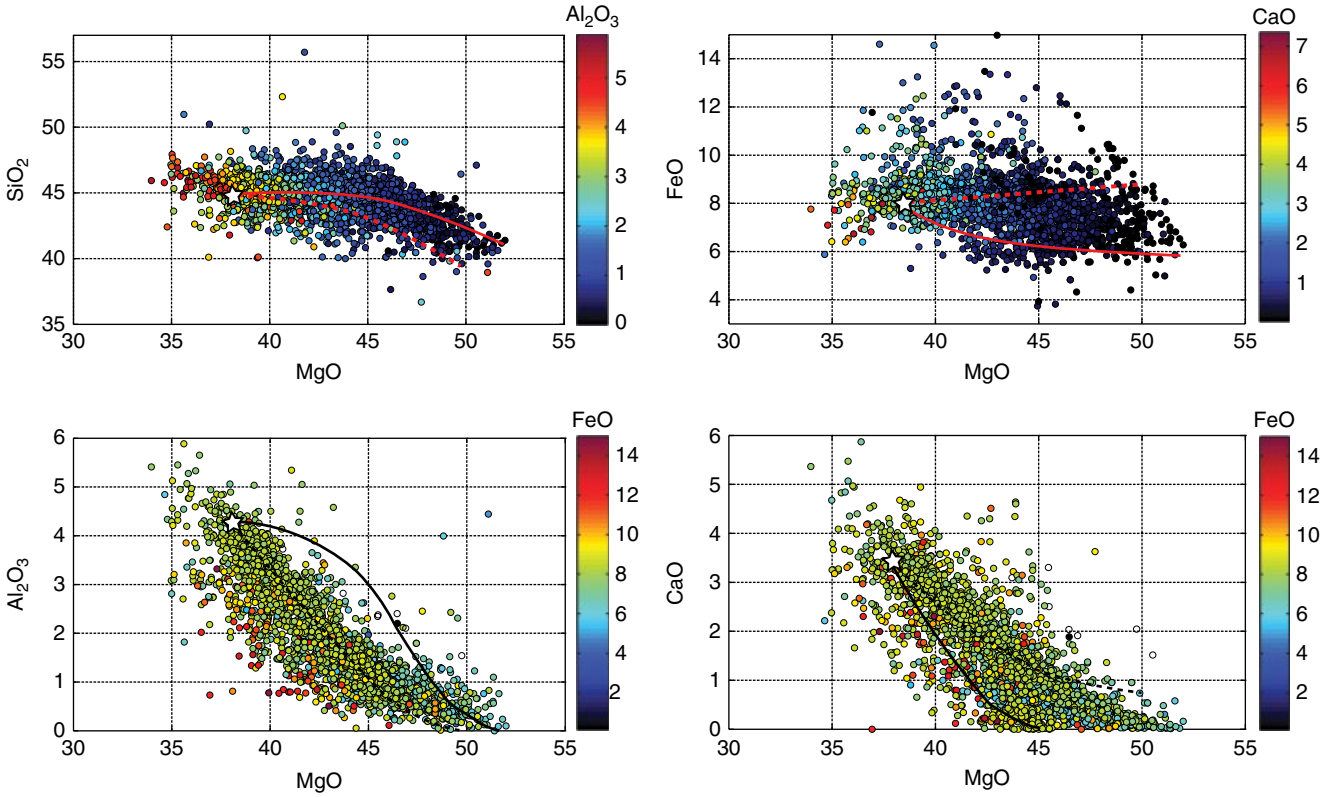

Figure 10.3 Covariation plots for a large database of mantle samples (e.g., xenoliths, abyssal peridotites, orogenic peridotites, etc.) showing the wide compositional range observed in natural samples. The color scales represent the content of a third oxide. Two polybaric perfect fractional melting paths [*Herzberg*, 2004] with different initial pressures of melting are included for comparison (*dashed line* = 2 GPa, *solid line* = 7 GPa). The initial fertile composition for these melting paths is indicated by the white star. After *Afonso et al.* [2013a].

difficult to constrain, but there is some agreement that their *average* volumetric proportions should not be higher than a few percent (e.g., see *Schulze* [1989], *Griffin and O'Reilly* [2007], and *Downes* [2007]). Even in such small amounts, eclogites can have a significant effect on some geophysical observables and mechanical properties of the lithosphere if they are concentrated at specific depths [*Griffin and O'Reilly,* 2007]. Unfortunately, their detection with geophysical techniques is still subject to large uncertainties.

Besides the presence of other ultramafic rocks, there is now abundant evidence of large compositional variability at different scales (vertical and lateral) within the peridotitic component of the lithospheric mantle [Figure 10.3; cf. *Carlson et al.* [2005], *Griffin et al.* [2009], *Bodinier and Godard* [2003], *Pearson et al.* [2003], and *Walter* [2003]). Since peridotites are thought to be the most important component by volume in the upper mantle, and their composition can inform on the origin, evolution, and bulk physical properties of the lithosphere, compositional variability within this group is of particular relevance. The terms "depleted" and "fertile" have become standard when describing the degree to which the composition of a mantle peridotite has been modified, relative to some assumed starting composition, by melt extraction and/or metasomatism. Highly depleted rocks can be significantly less dense and generally seismically faster than their fertile counterparts (cf. *Jordan* [1988], *Lee* [2003], *Anderson and Isack* [1995], *Schutt and Lesher* [2006], *Matsukage et al.* [2005], *Afonso et al.* [2010], and *Afonso and Schutt* [2012]). This is due to the transfer of specific chemical elements from the solid aggregate to the melt phase (i.e., incompatible elements), which is subsequently removed from the system. For instance, SiO_2, CaO, and Al_2O_3 are preferentially removed from the solid aggregate when melting occurs, while MgO tends to remain in the solid residue, and therefore its relative abundance increases in the solid. The behavior of FeO is more intricate, particularly at low pressures ($P < 3$ GPa; see *Afonso and Schutt* [2012]), but it generally decreases or increases at a smaller rate than MgO [*Herzberg*, 2004; *Kinzler and Grove*, 1992] during partial melting. Despite

second-order discrepancies between different melting models/experiments, the general "depletion pattern" of the five main oxides SiO_2–Al_2O_3–MgO–FeO–CaO is well understood, and their atomic ratios are typically used to quantify the degree of depletion in peridotites (cf. *Pearson et al*. [2003] and *Walter* [2003]). Amongst these, the ratio between MgO and FeO or "magnesium number" (Mg# = MgO/[MgO + FeO]), is of particular interest because (i) together with SiO_2, FeO and MgO typically account for more than 95% by weight of peridotites and thus exert a major control on modal compositions, (ii) these elements have a distinctive behavior during melting episodes that informs about the extent of partial melting (see below), (iii) MgO and FeO's strong influence on the relative abundances of mineral end-members of volumetrically dominant mineral phases (e.g., olivine and pyroxenes), and (iv) MgO and FeO's affect significantly the physical properties of the aggregate. During melt extraction, the Mg# of the residue increases almost linearly with degree of melting, regardless of whether melting is a batch or a fractional process and/or whether it occurs under wet or dry conditions [*Hirose and Kawamoto*, 1995; *Herzberg and O'Hara*, 2002; *Herzberg*, 2004]. Also, mainly due to (i) and (iii) above, there is a strong correlation between the residue's Mg# and its bulk density, shear-wave velocity, electrical conductivity, and compressional shear velocity (e.g., see *Speziale et al*. [2005], *Matsukage et al*. [2005], *Jones et al*. [2009], and *Afonso et al.* [2010]). The reader is referred to *Afonso and Schutt* [2012] and *Afonso et al*. [2013a] for thorough discussions of these topics in the context of geophysical studies.

The interpretation of the Mg# is less clear when pervasive metasomatism by infiltration of mafic melts take place [*Griffin et al*., 2009]. This is expected to occur in the deeper parts of the lithospheric mantle, which can be affected and modified by interaction with small amounts of melts produced in the asthenosphere (e.g., see *Tang et al*. [2006] *Piccardo* [2008], and *O'Reilly and Griffin* [2010, 2013]). When this occurs, FeO can be re-introduced into the solid assemblage during metasomatism by infiltration of mafic melts [*Griffin et al*., 2009], resulting in an overall reduction of the residue's Mg#. CaO and Al_2O_3 are also commonly added to the system by such processes. The metasomatic reintroduction of incompatible elements back into the depleted residue is referred to as "refertilization". Indeed, there is geochemical and geophysical evidence suggesting that large volumes of lithospheric mantle have been refertilized through percolation of melts (cf. *Chen et al*. [2009], *Pinto et al*. [2010], *Le Roux et al*. [2007], *Zheng et al*. [2007], *Griffin et al*. [2009], *Tang et al.* [2013], and *O'Reilly and Griffin* [2013]). Therefore, the Mg# of peridotites should not be seen as a measure of melt depletion only, but as an overall indicator of depletion and refertilization processes over time. Moreover, cautions should be exercised when making assumptions about the average Mg# of the subcontinental mantle based on the age of the overlying crust, as it is now well-known that this is not a global pattern [*Griffin et al*., 2009; *O'Reilly and Griffin*, 2013].

If the lithosphere is indeed isolated from the homogenizing process of high-temperature convection, it should accumulate and preserve distinct geochemical and isotopic signatures for longer periods than the underlying convecting mantle. Indeed, trace-element and isotopic studies in mantle peridotites have provided crucial information on the nature and time scale of melting and metasomatic events (e.g., see *Hofmann* [1997] and *Stracke and Bourdon* [2009]). However, the effects of trace elements on geophysically relevant properties of mantle rocks is negligible. A significant exception is water, which exerts a major influence on some important properties of mantle rocks, even when present in trace (ppm) amounts (e.g., see *Karato and Jung* [1998], *Karato* [2008], and *Yoshino and Katsura* [2013]). Water is two to three orders of magnitude more soluble in melts than in mantle minerals (cf. *Hirschmann* [2006]). Consequently, considering typical water contents in mantle rocks (<200–300 ppm wt%), melt extractions of only <10% can effectively "dry out" the residue, significantly increasing its electrical resistivity and viscosity relative to its hydrated counterpart (e.g., see *Karato* [1986], *Hirth and Kohsltedt* [1996], *Karato* [2008], and *Jones et al*. [2012]). Furthermore, it has been recently suggested that water can also significantly affect seismic attenuation and velocities by increasing the effect of the dissipation peak due to grain-boundary sliding [*Karato*, 2012]. This hypothesis is consistent with a limited number of experimental results (e.g., *Aizawa et al*. [2008]) and helps reconciling some contradictory seismological observations that are difficult to explain in terms of our current state of knowledge regarding the temperature and water effects on seismic observables.

In summary, there is now abundant evidence that the lithospheric mantle is highly heterogeneous, both in composition and structure. Although single-data or stand-alone approaches have been successful in providing the long-wavelength pattern of lithospheric structure (see above), imaging the fine-scale thermochemical structure of the lithosphere with geophysical techniques remains a challenging, yet crucial, problem. Some of the difficulties are technical/methodological in nature (e.g., insufficient computer power, inefficient algorithms, biased prior information, etc.) or related to incomplete/poor data (e.g., lack of dense high-resolution datasets, incomplete mineral physics data, etc.) and are therefore amendable in principle. However, a significant part of the problem is related to its actual physical nature and thus intrinsic to the problem of retrieving the physical state of the Earth's interior from indirect measurements (Section 10.5).

10.4. SINGLE-DATA AND MULTI-OBSERVABLE APPROACHES

Geophysical methods used to image the lithospheric and upper mantle structure have improved dramatically in the past 30 years due to rapid advances in both computing power and data acquisition/processing techniques (cf. *Romanowicz* [2003], *Rawlinson et al*. [2010], *Liu and Gu* [2012], *Kuvshinov and Semenov* [2012]). Quite naturally, these methods evolved largely in isolation from each other, each focusing on the treatment of a specific dataset. Some of the most common single-data approaches used to study the lithosphere and upper mantle include teleseismic tomography (e.g., see *Evans and Achauer* [1993], *Granet et al*. [1995], and *Rawlinson et al*. [2006], surface-wave tomography (e.g., see *Pasyanos and Nyblade* [2007], *Yang et al*. [2008], *Fishwick et al*. [2008], and *Agius and Lebedev* [2013]), gravity modeling (e.g., see *Zeyen and Fernàndez* [1994], *Torne et al*. [2000], *Ebbing et al*. [2006], *Chapell and Kusznir* [2008], *Tašárová et al.* [2009]), electromagnetic methods (e.g., see *Heinson* [1999], *Jones* [1999], *Jones et al*. [2009a], *Evans et al*. [2005], *Evans et al*. [2011], and *Meqbel et al*. [2014]), local earthquake tomography (e.g., *Aki and Lee* [1976], *Eberhart-Phillips* [1990], and *Kissling et al*. [1994]), and receiver function studies (e.g., *Yuan et al*. [2006], *Kawakatsu et al*. [2009], *Rychert and Shearer* [2011], and *Kind et al*. [2012]). The first four are of particular relevance to us, as they are most sensitive to the shallow mantle structure, they offer complementary information and resolutions, their datasets are amenable to well-known inversion/modeling methods, and they are not restricted to seismogenic regions (as is local earthquake tomography). In addition, a number of studies have successfully combined them (in pairs) in joint inversions for crustal, lithospheric, and upper mantle structure in general. The most common example, and perhaps the most mature in terms of methodology, is that of joint inversion of body-wave and surface-wave data (e.g., see *West et al*. [2004], *Rawlinson and Fishwick* [2011], and *Obrebski et al*. [2011]). However, attempts to combine magnetotelluric (MT) data and surface waves [*Moorkamp et al*., 2010; *Roux et al*., 2011; *Vozar et al*., 2014], receiver functions and MT data [*Moorkamp et al*., 2007], surface waves and receiver functions [*Julia et al*., 2000; 2003; *Tkalčić et al*., 2006], and gravity and body waves (e.g., see *Zeyen and Achauer* [1997] and *Tiberi et al*. [2003]) have also yielded promising results (see Section 10.4.1) and will undoubtedly become the subject of further research.

The need for combining different datasets when studying the structure of the lithosphere and upper mantle is straightforward to understand and justify. *Afonso et al*. [2013a] recently provided an extensive discussion of the benefits (and difficulties) of working with multiple observables for this purpose. The main objective of inverting/modeling multiple geophysical observables is twofold: Firstly, we aim at minimizing the range of acceptable models by adding additional constraining data (i.e., reduce the space of valid solutions). Secondly, we try to gain additional information on the problem at hand (i.e., obtain "more comprehensive" models) by adding observations with different sensitivities to different aspects of the problem. For instance, while short-period surface-wave data offers good resolution at shallow depths (where teleseismic ray paths do not cross) and provide information on the absolute velocity structure beneath the array, body-wave data can add critical information on deeper features (provided the array has a large aperture) and improve lateral resolution [*Rawlinson and Fishwick*, 2011; *Obrebski et al*., 2011]. It is therefore not only desirable but also necessary that each new observable added to the inversion/modeling have a different sensitivity to the model parameters of interest. This seemingly obvious requirement is crucial when the uncertainties in observations are formally considered. Every new observable carries uncertainties that are propagated to the final result (cf. *Tarantola* [2005]). Therefore, if a new observable is added to the inversion, but its sensitivity is similar to or less than that of the existent data, the net effect could be a degradation of the results (uncertainty is added, but not new constraints).

10.4.1. Topography and Gravity Field Modeling

To the first order, and disregarding dynamic contributions, the elevation (i.e., topography and bathymetry) of the Earth's surface is a measure of the buoyancy (average density) of the lithosphere [*Lachenbruch and Morgan*, 1990]. Local isostasy is one of the oldest principles in geophysics and has been proven to be a suitable approximation for explaining topographic loads with wavelengths $\gtrsim$100 km [*Turcotte and Schubert*, 2014; *Lachenbruch and Morgan*, 1990; *Watts*, 2011; *Hasterok and Chapman*, 2007]. According to the principle of isostasy in its most popular form, all regions of the Earth with identical elevation must have the same buoyancy (mass per unit area) when referenced to a common compensation level. Although there is no perfect compensation level in the Earth's mantle (temperature and pressure disturbances associated with convective flow prevent its existence), it can be shown that in a mantle-like fluid, surface topography is primarily controlled by temperature (density) variations in the vicinity of the upper thermal boundary layer (i.e., lithosphere) and is relatively insensitive to thermal (density) anomalies below a certain critical isotherm [*Parsons and Daly*, 1983]. Therefore, absolute elevation can be used as a constraint to possible density structures within the lithosphere (e.g., see *Sclater and Francheteau*, [1970], *Turcotte and Schubert* [2014],

Lachenbruch and Morgan [1990], and *Hasterok and Chapman* [2007, 2011]). This principle is commonly referred to as "lithospheric" or "thermal isostasy".

Gravity-related observables are sensitive to subsurface mass anomalies, but their inversion alone for the density distribution within the Earth is an ill-posed and non-unique problem. Further constrains can be added to the modeling/inversion of gravity considering the temperature dependence of mantle density through thermal expansion. This normally involves joint modeling/inversion of gravity data together with an extra observable directly related to thermal structure and independent from density variations: the surface heat flow (e.g., see *Zeyen and Fernàndez* [1994], *Fullea et al*. [2007], and *Jiménez-Munt et al*. [2010]). Unfortunately, surface heat flow tends to be dominated by crustal effects (e.g., radiogenic heat production, groudwater flow, etc.), which need to be properly taken into account when modeling lithospheric geotherms [*Jaupart and Mareschal*, 2011; *Furlong and Chapman*, 2013]. Also, since both topography and gravity field observables (i.e., gravity and geoid anomalies, gravity gradients) depend upon the density distribution within the Earth, in principle they can be jointly modeled (e.g., see *Fernàndez et al*. [2004] and *Zeyen et al*. [2005]) or inverted (e.g., see *Fullea et al*. [2007] and *Kumar et al*. [2014]) to obtain estimates of the lithospheric structure. However, care must be taken in regions where large sublithospheric dynamic effects may be present (e.g., see *Hager and Richards* [1989], *Forte* [2007], *Afonso et al.* [2008b], *Khan et al*. [2013], and *Shan et al*. [2014], as they can introduce systematic errors in the modeled lithospheric structure.

Gravity anomalies (Bouguer, free air) are typically used to constrain crustal densities and geometries (e.g., see *Ebbing et al*. [2006], *Chapell and Kusznir* [2008], *Torne et al*. [2000], and *Fullea et al*. [2008]). Geoid anomalies are affected by mass/density anomalies over a wider range of depths than gravity anomalies (e.g., see Bowin [2000]). Therefore, appropriate wavelength filtering of the geoid anomaly allows studying the Earth at different scales, from the crust (e.g., see *Doin et al*. [1996] and *Sandwell and MacKenzie* [1989]) to the deep mantle (e.g., see *Hager* [1984], *Ricard et al*. [1984], *Forte and Mitrovica* [2001], and *Deschamps et al*. [2001]). Satellite gravity data are a unique source of information on the density structure of the Earth due to its global and relatively uniform coverage. The recent GOCE (Gravity field and steady-state Ocean Circulation Explorer) satellite mission (launched in 2009) included, for the first time, an on-board three-axis gradiometer able to measure the Earth's gravity gradients at satellite height (e.g., see *Pail et al*. [2011]). This new type of gradiometric satellite measurement is more sensitive to spatial structure and directional properties of the Earth's internal density distribution than classic observations on gravitational intensity (gravity and geoid anomalies). In contrast to terrestrial gravity gradients (characterized by a high-frequency content related to near-surface structures), the gradiometric tensor measured in the local satellite framework (255 km on average for GOCE) is naturally filtered, retaining the lithospheric and underlying mantle density signal. Pioneering recent studies have showed very promising results in imaging the Earth's crust [*Reguzzoni et al.*, 2013] and mantle density structure using this new type of data [*Panet et al.*, 2014; *Fullea et al.*, 2015], although its full potential is yet to be fully exploited.

10.4.2. Joint Inversions of Seismic Data

Teleseismic travel time tomography is one of the most widely used techniques to image the 3D velocity structure of the lithosphere and uppermost upper mantle (cf. *Evans and Achauer* [1993] and *Rawlinson et al*. [2010]). Its popularity resides in the relatively low cost of passive seismic deployments, the high horizontal resolution (on the scale of tens of kilometers) that can be achieved, its applicability to regions with no local seismicity, and the high-quality data that can be extracted from the array using cross-correlation techniques (e.g., see *VanDecar and Crosson* [1990], *Evans and Achauer* [1993], and *Rawlinson and Kennett* [2008]). However, despite the many benefits of teleseismic travel-time tomography, there are some important limitations that need to be considered when interpreting tomographic images obtained with this technique. Two of the most important limitations when studying the structure of the lithosphere and upper mantle are the lack of information on absolute velocities and the lack of resolution of the shallow structure beneath the array (cf. see *Evans and Achauer* [1993] and *Foulger et al*. [2013]). The first of these limitations is due to the fact that, in order to mitigate biases associated with uncertainties in source parameters (i.e., hypocenter location and origin time) and large-scale heterogeneities along the path between the source and the receiver, only *relative* travel time residuals are used in the inversion. As a consequence, only *relative* wave speeds can be recovered and the actual amplitudes of the variations are typically underestimated. The second limitation is a consequence of using teleseismic events, which results in ray paths that are sub-vertical when they arrive at the array, resulting in poor ray crossing at shallow depths beneath the array.

One way to overcome (or at least minimize) these limitations is to include information from surface wave data. Several variations of this general recipe have been used in the literature to obtain high-resolution models of velocity structure above the mantle transition zone (e.g., see *West et al*. [2004], *Rawlinson and Fishwick* [2011], and

Obrebski et al. [2011]). Phase-velocity dispersion maps obtained from the combination of ambient noise tomography with teleseismic surface wave tomography constitute one of the best sources of information for retrieving absolute Vs values in the lithosphere and sublithospheric upper mantle (e.g., see *Yang et al.* [2008]). The main advantage of this method is that while ambient noise tomography (ANT) provides detailed information at short periods (shallow levels), teleseismic earthquake methods such as multiple-plane-wave tomography provide the complementary information at longer periods (deep levels). The ability to recover "good" values of Vs, however, depends on the uncertainties associated with the phase-velocity dispersion maps generated by each method. The combination of surface and body wave data in joint inversions will likely be boosted by (1) the recent advances in ambient noise tomography to obtain short and long period phase-velocity information, (2) the popularization/optimization of Monte Carlo approaches to invert for velocity structure, and (3) the rapidly growing seismic infrastructure and deployment of dense arrays around the globe (e.g., USArray, IberArray, ChinArray, etc.). This is an area with great (proven) potential to study the fine-scale velocity structure of the lithosphere and upper mantle. The inclusion of surface wave overtones into such joint inversions provides not only better resolution with depth but also additional (albeit weak) sensitivity to the Vp structure [*van Heijst and Woodhouse*, 1999]. This (information on both Vs and Vp) is particularly useful when making inferences about the thermochemical structure of the Earth [cf. *Khan et al.*, 2011; *Afonso et al.*, 2010, 2013a].

Joint inversions of surface wave and receiver function (RF) data are an attractive alternative to constrain the velocity structure of the first ~300 km of the Earth. While surface wave data provide essential constrains on the absolute 3D velocity structure, it cannot constrain simultaneously the strength and location of shear velocity discontinuities (e.g., Moho–mantle transition). This problem results in velocity models with high uncertainties around regions of sharp discontinuities. RFs, on the other hand, are highly sensitive to velocity discontinuities beneath the station, particularly to the Moho discontinuity, but not to the absolute velocity structure due to a depth–velocity trade-off [*Ammon et al.*, 1990]. Following the pioneering work of *Julia et al.* [2000] using P-wave RFs and dispersion data, many authors have successfully used this approach to study crustal and shallow mantle structures (e.g., see *Lawrence and Wiens* [2004], *Tkalčić et al.* [2006], and *Shen et al.* [2013]). The extension of this technique to constrain the whole lithospheric structure, however, still is in its infancy, and further studies are needed to show its general applicability and reliability. To this respect, the joint inversion of S-wave RFs and long period dispersion data represents a promising, yet understudied, approach. The advantage of using S-wave RFs is that deeper signals associated with LAB structure are less susceptible to contamination by crustal and deeper reverberations [*Yuan et al.*, 2006], which constitute a major difficulty when working with P-wave RFs (cf. *Kind et al.* [2012] and *Chen et al.* [2009]). Despite this advantage, S-waves usually have a larger noise–signal ratio than P-waves and are characterized by lower frequencies (due to stronger attenuation at higher frequencies). Therefore, S-wave RFs are not well suited to resolve details about the crustal structure beneath the station. Therefore, while the use of S or P-wave RFs in joint inversions is dependent on the goals of the study, the joint inversion of S and P-wave RFs with surface wave data is an attractive possibility that holds some potential to obtain detailed seismic images of the lithosphere.

10.4.3. Joint Inversions of Electromagnetic (EM) and Seismic Data

Traditionally, deep EM studies have used time series of the magnetic field variations recorded on the global network of geomagnetic observatories to infer the Earth's electrical conductivity. 1D geomagnetic deep soundings and horizontal spatial gradient studies [e.g., *Fuji and Schultz*, 2002; *Olsen*, 1999] and 3D inversion of geomagnetic observatory data [e.g., *Kelbert et al.*, 2009; *Tarits and Mandea*, 2010; *Semenov and Kuvshinov*, 2012] constrain the conductivity distribution in the mantle in the depth range 400–1600 km (i.e., periods of few days to few months). Long-period magnetotelluric (MT) responses (magnetic plus horizontal electric field component) cover complementary periods up to few days, sampling upper mantle depths (<400 km). However, high-quality long-period MT data (periods <10 days) are difficult to obtain due to technical and intrinsic limitations of the method [*Shimizu et al.*, 2010]. On top of that, the biggest limitation of observatory data is their poor coverage of the Earth's surface (sparse distribution over continents and almost nothing over oceans) that severely hampers the robustness and accuracy of global EM models. Satellite measurements represent an attractive alternative to the sparse terrestrial observatory data, providing high-precision and high-resolution magnetic field measurements with uniform global coverage (e.g., see *Sabaka et al.* [2004] and *Olsen et al.* [2013]). Recent advances in global 3D EM (spherical) forward modeling, the increasing availability of computational resources, and satellite data have made it possible to obtain a new generation of global electrical conductivity models of the mantle. Electromagnetic perturbations of ionospheric source (Sq) derived from satellite data are sensitive to the lithosphere–uppermost

mantle conductivity structure (depth: 100–400 km; cf. *Koch and Kuvshinov* [2013]). The conductivity structure in the lower mantle can be derived from the inversion of time series of internal (induced) and external (inducing) spherical harmonic expansion coefficients related to disturbed storm-time variations of magnetospheric ring current origin (Dst) (time and frequency approaches; cf. *Velimskỳ* [2013] and *Püthe and Kuvshinov* [2014]). A common caveat associated with most EM inversions is that while they predict perfectly valid resistivity models, these models are not necessarily directly related to the actual thermochemical structure inside the Earth due to resolution and uncertainty issues. For example, although for a 1D Earth there exists a uniqueness theorem for perfect data at all frequencies [*Bailey*, 1970], data insufficiency and inaccuracy lead to highly nonlinear resolution of model parameters. In particular, the true resistivity of a resistive layer or region beneath a more conducting one is very difficult to resolve due to the screening effect of the upper layer. Thus, only a lower bound on the resistivity of the mantle directly below the crust can usually be set [*Jones*, 1999].

More than 15 years ago, *Jones* [1998] showed a variety of examples where joint interpretation of collocated seismic and magnetotelluric (MT) measurements led to more robust inferences about structures and processes within the lithosphere, partially mitigating the inherent uncertainties associated with EM inversion. Since then there has been a steady, but relatively small, number of studies that formally make use of both datasets (e.g., see *Snyder et al*. [2004], *Jones et al*. [2009b], *Jones* [1998] and *McGary et al*. [2014]). New interdisciplinary initiatives such as Earthscope [*Meltzer*, 2003] provide ample opportunity for more formal combinations of seismic and electromagnetic measurements.

So far, there have been successful examples of joint modeling (see below), and the widespread use of structural constraints (see Chapter 4) utilized in near-surface (Chapter 7), mining (Chapter 8), and hydrocarbon applications (Chapter 9) demonstrates that it is possible to generate useful joint inversion results even without precise knowledge of the physical properties of the different minerals. In the following we will give an overview of the first attempts that have been made to combine MT and seismic data to study the lithosphere–asthenosphere system. We will focus on quantitative approaches that move beyond simple comparisons of images. These include both simultaneous joint inversion and modeling as well as structural classification based on independent inversions.

To the best of our knowledge, the only joint inversion study of MT and seismic data with real data that focuses on the structure of the crust, and that has not been covered in any of the other chapters, has recently been published by *Bennington et al*. [2015]. These authors combine double-difference tomography [*Zhang and Thurber*, 2003] with a 2D MT modeling algorithm based on OCCAM2D [*Constable et al*., 1987]. To couple velocity and conductivity they use a modified version of the cross-gradient constraint they call the "normalized cross-gradient" where they normalize the components of the gradient by the total length of the gradient vector before calculating the cross product. This normalization enhances the influence of regions in the model where one or both of the gradients in velocity and conductivity are small. Their synthetic tests with realistic acquisition geometries and noise comparable with field data demonstrate that the joint inversion produces significantly better results even though it might not be visually obvious at first glance. Similarly, the overall appearance of the individual inversion results and the joint inversion results is quite similar.

Bedrosian et al. [2007] outline a possible strategy for identifying lithological variations across a fault zone based on a post-inversion structural classification of resistivity and velocity models. Some of the technical details of their approach are discussed in Chapter 5. Even though the two models have been obtained independently and thus similarity between the models has not been enforced in the inversion, they demonstrate that their method produces spatially coherent clusters that correspond to known and assumed geological formations. Compared to a full joint inversion of the seismic and MT data, the advantage of the post-inversion approach is that it can be applied to models generated by different researchers at different times. Also, different classification approaches could be used without having to modify the existing inversion algorithms. A potential disadvantage compared to joint inversion is that there is no exchange of information on structural boundaries. In some cases this could result in overly blurry boundaries between different lithological classes. For the results presented by *Bedrosian et al.* [2007], however, this does not seem to be a major issue.

Most studies combining seismic and MT data in a joint inversion and looking at the whole lithosphere and the asthenosphere are based on the methodology described in *Moorkamp et al*. [2007, 2010] and are limited to simple one-dimensional geometries. *Moorkamp et al*. [2010] invert magnetotellurics, receiver functions, and surface wave dispersion data to determine conductivities, shear wave velocities, and layer thicknesses for a layered Earth (Figure 10.4). In Figure 10.4 we can see how the layer interfaces for the electric and seismic model coincide for each site as coincident layer interfaces couple the electric and seismic parameters. For this type of approach, this is an essential step to ensure adequate coupling. If there are too few layers, it is not possible to explain both datasets

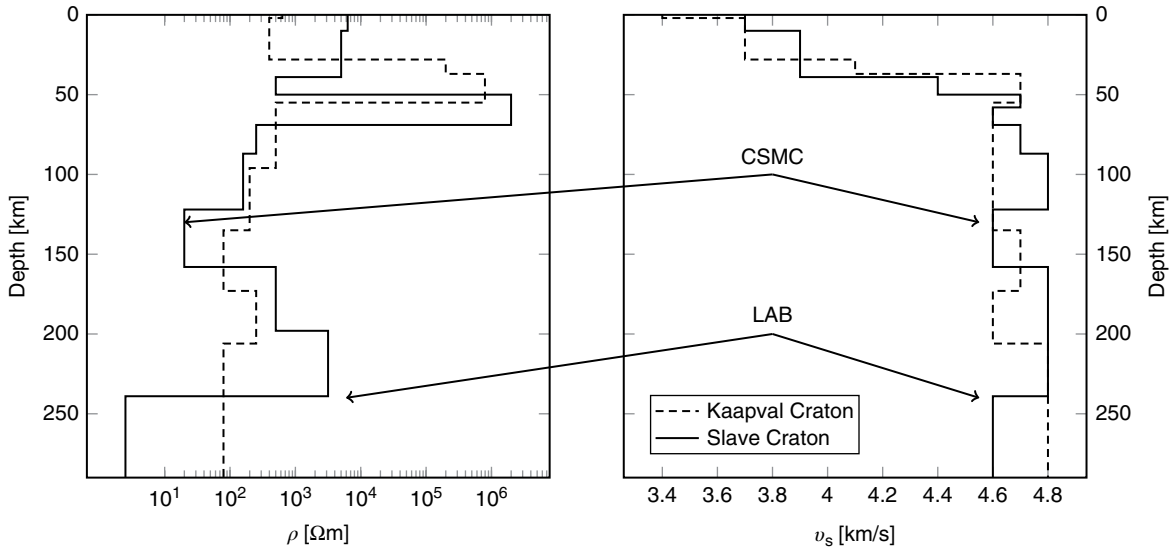

Figure 10.4 Comparison of the joint inversion results for the Kaapvaal Craton (*dashed line*) and the Slave Craton (*solid line*). We show resistivity on the left and velocity on the right-hand side. The results for the Slave Craton show a clear lithosphere–asthenosphere boundary (LAB) and a mantle conductor (CSMC) associated with a low-velocity zone. The Kaapvaal Craton shows some similar features; however, their expression is less pronounced, possibly because of lower data quality.

simultaneously. If there are too many layer, there is no coupling between the seismic and electromagnetic methods.

Roux et al. [2011] show an extension of the approach discussed above to 1D anisotropic structures. The motivation for developing this approach was the observation of coincident directions of anisotropy at similar depths in independently generated surface wave [*Lebedev et al*., 2007] and MT [*Gatzemeier and Moorkamp*, 2005] models. Thus one of the aims of this study was to quantitatively investigate the hypothesis that the directions and depth ranges of the electric and seismic anisotropy can be modelled as coincident within the resolution of the data. This is one of the predictions made by the hydrogen diffusion argument [*Gatzemeier and Tommasi*, 2006] sometimes employed to explain electrical anisotropy in the asthenosphere (e.g., see *Poe et al*. [2010] and *Dai and Karato* [2014]). The joint inversion results agree with this hypothesis and retrieve two main regions of anisotropy. The resistivities in the asthenosphere differ by a factor of ten between the most conductive and most resistive direction. This is one order of magnitude lower than the previously inferred factor of 100 [*Gatzemeier and Moorkamp*, 2005] and agrees with the values expected from hydrogen diffusion [*Simpson and Tommasi*, 2005]. A subsequent study by *Mandolesi and Jones* [2014] using MT inversion constrained by a seismic model yields slightly different results, but confirms the essential conclusions of an anisotropic asthenosphere.

The above discussion has illustrated some of the strengths, but also some severe limitations of joint inversion of EM and seismic data for the crust and mantle structure in its current form. Structural constraints can be employed, as a priori information, to retrieve coincident structures (i.e., electrical conductivity and seismic velocity) under general assumptions as a first-order estimate. The more powerful, but also more computationally restrictive, geophysical–petrological approach is based on the experimental and thermodynamic relationship between physical properties of rocks (seismic, electric) and the subsurface thermochemical structure (e.g., see *Fullea et al*. [2011], *Khan and Shankland* [2012], and *Vozar et al*. [2014]). The electrical conductivity of the major upper mantle mineral phases (e.g., olivine, pyroxenes, garnet) can be described as an activated process in a semiconductor and, therefore, characterized by an Arrhenius-type power law. The conduction mechanism changes at around 1300–1500°C from small polaron at $T < 1300$°C to ionic conduction. The bulk or whole rock conductivity can be determined according to the individual contribution of its mineral phase constituents (including the presence of interconnected amounts of water and melt) using an appropriate mixing theory (e.g., see *Xu et al*. [2000], *Ledo and Jones* [2005], *Fullea et al.* [2011],and *Khan and Shankland* [2012]). In order to model consistent amounts of water in the mantle, it is important to constrain, based on laboratory studies, (i) the water storage capacity or solubility for the major mineral phases and (ii) the partition coefficient or solubility ratio

of water for the different minerals. The solubility reflects the maximum possible water content that a mineral, or an assemblage of minerals, can accommodate within their structures without saturating or producing a water-rich fluid or hydrous melt at a given pressure, temperature, and composition (e.g., see *Mierdel et al*. [2007] and *Ferot and Bolfan-Casanova* [2012]). The partition coefficients characterize the relative proportion of water among the different phases in the assemblage (e.g., see *Dai and Karato* [2009], *Ferot and Bolfan-Casanova* [2012], and *Novella et al*. [2014]). Values for partition coefficients estimated from measurements in natural samples (e.g., see *Kovács et al*. [2012] and *Grant et al*. [2007]) and laboratory studies (e.g., see *Dai and Karato* [2009], *Aubaud et al*. [2004, 2008], and *Kovács et al*. [2012]) show considerable variability. Experimental studies also show, with considerable scatter in the values, a significant variation (up to two orders of magnitude) of partition coefficients with variations in temperature (e.g., see *Dai and Karato* [2009]), pressure (e.g., see *Novella et al*. [2014]) and water content (e.g., see *Dai and Karato* [2009]).

In contrast to seismic velocities, which are mostly sensitive to bulk physical properties, electrical conductivity is strongly affected by interconnected minor constituents (e.g., water, volatiles, or melt) with a large influence on the rheological–dynamic behavior of the Earth. The effect of water, in particular, is a matter of heated debate (e.g., see *Karato* [2011] and *Dai and Karato* [2014]), with estimates of its distribution within nominally anhydrous magnesium-silicate mantle minerals (NAMs) also uncertain (e.g. see *Jones et al*. [2012]). In spite of their characterization as anhydrous, NAMs (e.g., olivine, wadsleyite, ringwoodite, pyroxenes) can host significant amounts of (structurally bounded) water in their crystal structure based on experimental solubility studies (e.g., see *Bolfan-Casanova et al*. [2000]).

Vozar et al.'s [2014] 1D joint modeling of long-period surface-wave phase velocities, MT responses and surface topography in central Tibet (Qiangtang and Lhasa terranes) is based on a self-consistent petrological–geophysical thermodynamic framework where mantle properties are calculated as a function of temperature, pressure, and composition. Long-period surface-wave phase velocities are most sensitive to seismic wave speeds and, through them, to temperature within the lithosphere and sublithospheric mantle. In contrast, surface waves are only weakly sensitive to small amounts of water, which has a large impact in MT data along with temperature. Surface topography senses the average lithospheric density distribution, the latter being affected by the geotherm and bulk composition. In the northern Qiangtang terrane, these authors find a dry 80-120-km-thick lithosphere associated with a relatively fertile composition (garnet lherzolite), as commonly present in Asian mantle xenolith data (Figure 10.5). In contrast, in the southern Lhasa terrane, the LAB depth is about 180 km, with an additional requirement of a moderate amount of water in the lithospheric mantle (<0.02 ppm wt%). The mantle composition modeled in Lhasa is compatible with phlogopite-bearing Fe-rich spinel harzburgite rocks from xenoliths erupted in West Lhasa, suggesting metasomatism (e.g., Fe-enrichment of a previously depleted mantle) and rehydration as evidenced by the hydrous mineral phases [*Vozar et al*., 2014]. The complementary sensitivities of the different data types modeled by *Vozar et al*. [2014] allows putting tight constraints on the thermochemical structure and hydrous state of the lithosphere, overcoming the limitations, restrictions, and inconsistencies of separate modeling of the different datasets.

The current 1D joint approaches integrating EM and seismic datasets can only capture a crude picture of the true structure of the Earth's subsurface. Although valid under some conditions, the assumption of a layered Earth is less appropriate in areas where large lateral heterogeneity plays an important role. This dimensional limitation will be overcome once 3D joint inversion approaches on this scale become available. Significant efforts have been devoted to connect EM and other geophysical datasets with the subsurface thermochemical structure (e.g., see *Fullea et al*. [2011], *Jones et al*. [2012], *Khan and Shankland* [2012], *Koyama et al*. [2014], *Vozar et al*. [2014], *Khan et al*. [2015], and *Koyama et al*. [2014]), yet a full 3D joint inversion and/or modeling of global EM data—in particular, new satellite magnetic data with global and uniform coverage—for the thermochemical structure in the lithosphere is still to come. Combining a thermochemical/experimental EM approach with other geophysical techniques in a relatively mature state (e.g., seismic, gravity field modeling/inversion), exploiting complementary sensitivities, is an important strand of research that will likely receive attention in the near future.

10.4.4. Integrated Modeling

Most of the preceding methods can be called "classic" or "traditional" in the sense that their main objective is to construct models of the distribution and magnitude of physical *parameters* inside the Earth, such as wave velocity, electrical conductivity, wave attenuation and bulk density, which are then used to make a posteriori (indirect) inferences about the physical state of the Earth's interior (i.e., temperature, pressure, composition). We refer to these methods as "*parametric methods*". Unfortunately, the interpretation of these parameters in terms of the physical state of the Earth's interior is often contentious and ambiguous. Indeed, this remains a major stumbling block in understanding exactly what is being imaged with tomography methods and what is the real geological significance of the imaged boundaries and 3D architecture

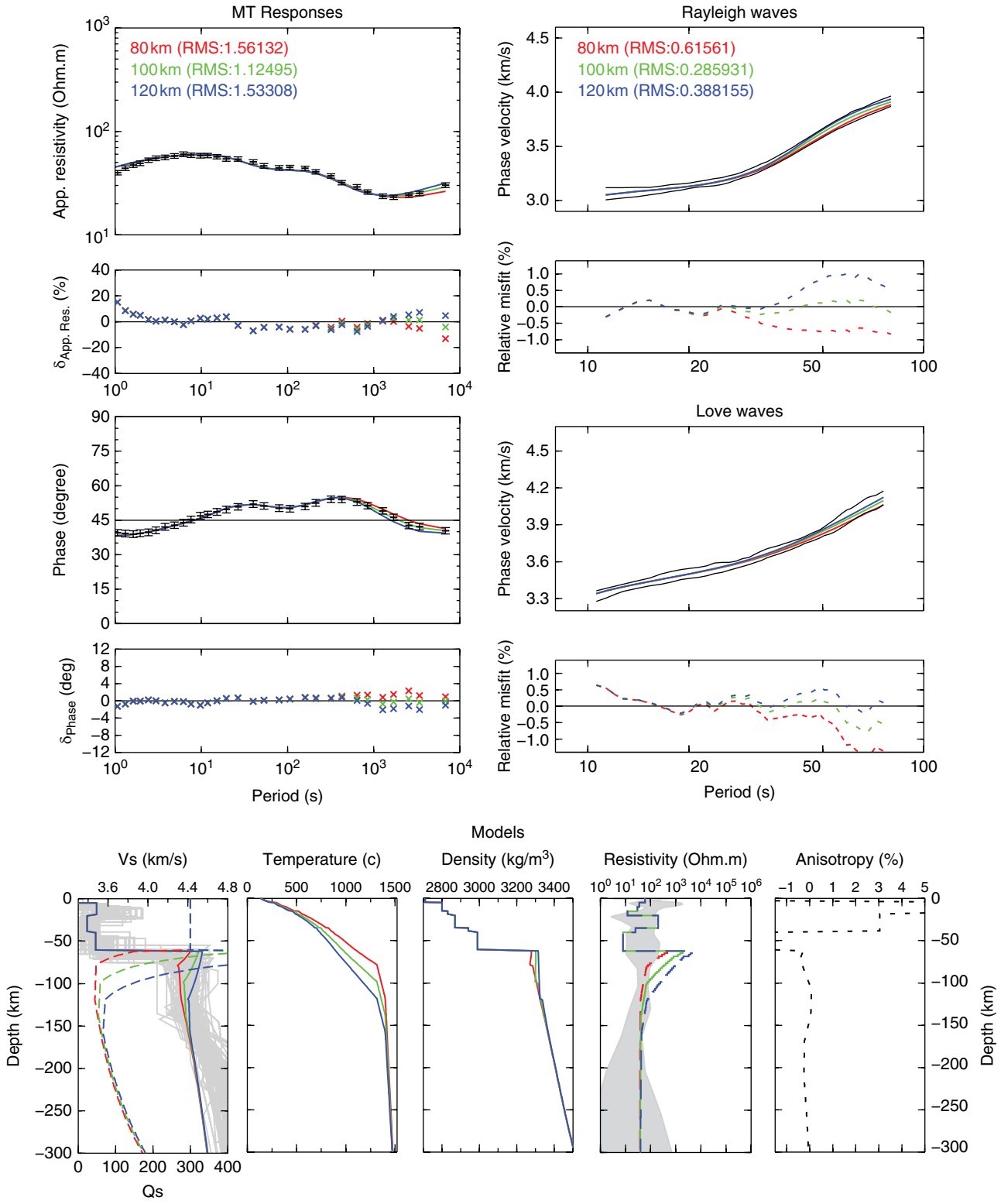

Figure 10.5 Integrated geophysical–petrological modeling of surface waves and MT dat. **(Top)** Fits of MT and seismic data for three (red 80 km, green 100 km, and blue 120 km) different LAB depths. **(Bottom)** Corresponding calculated models of Vs velocities (*dashed lines* represent shear-wave quality factors Qs, *gray lines* represent all possible models based only on seismic modeling), temperature, density, resistivity (*gray area* represents the range of all resistivity models based only on MT data), and anisotropy. After *Vozar et al.* [2014]).

(e.g., see *Afonso et al*. [2010, 2013a,b], *Foulger et al*. [2013], *Becker* [2012], and *Khan et al*. [2015]). In a strict sense, however, there is no real pressing need for knowing the distribution of, for example, wave velocity or electrical conductivity inside the Earth. What we ultimately require is the thermochemical structure of the planet, as this controls important near-surface processes (e.g., seismicity, magma emplacement, mineralization events, etc.), the expression of most geophysical observables (e.g., gravity, travel times, etc.), and the behavior and evolution of tectonic plates (e.g., plate velocity, strain partitioning, etc.).

An integrated approach specifically designed for forward thermochemical modeling of the lithosphere and uppermost mantle, including most available geophysical–petrological constraints, is represented by the LitMod suite [*Afonso et al*., 2008a; *Fullea et al*., 2009]. The LitMod suite is a set of 1D, 2D, and 3D self-consistent and interactive codes where all relevant mantle properties (e.g., density, electrical conductivity and seismic velocities) are functions of temperature, pressure, and bulk composition and obtained by Gibbs free energy minimization (e.g., *Connolly* [2009]) using well-known thermodynamic formalisms and internally consistent databases (e.g., see *Stixrude and Lithgow-Bertelloni* [2005, 2011] and *Holland and Powell* [2011]. These codes solve all the required forward problems (e.g., heat transfer, geopotential, electromagnetic, etc.) allowing to simultaneously fit multiple geophysical observations (e.g., elevation, heat flow, gravity potential fields, seismic and magnetotelluric data). When available, petrological data (e.g., amount of partial melting, compositional data from xenoliths, etc.) can be input into the model as well. Besides allowing for a better control of the lateral and vertical variations of the bulk properties, this method reduces the uncertainties associated with fitting each observable alone or in pairs, as commonly done in the literature, and explicitly considers modal (mineral volume fractions) and mineral compositional effects, complex solid–solid mineral phase transitions (and their associated entropy and latent heat changes), hydration effects/state, and, in some cases, melting. The reader is referred to *Afonso et al*. [2008a] and *Fullea et al*. [2009] for further details. This integrated forward methodology has been successfully applied to produce models of the lithosphere at a regional scale in different tectonic scenarios, from young Phanerozoic active zones (e.g., see *Fullea et al*. [2010], *Gradmann et al*., [2013], *Carballo et al*. [2015], *Vozar et al*. [2014], and *Pedreira et al*. [2015]) to old cratonic areas (e.g., see *Fernàndez et al*. [2010] and *Fullea et al*. [2011]) (Figure 10.6). As an example of a recent application of this approach, we refer to the study of *Gradmann et al*. [2013]. These authors studied the southwestern Fennoscandian thermochemical lithospheric structure using observed seismic velocities, gravity anomalies and topography data. Their results

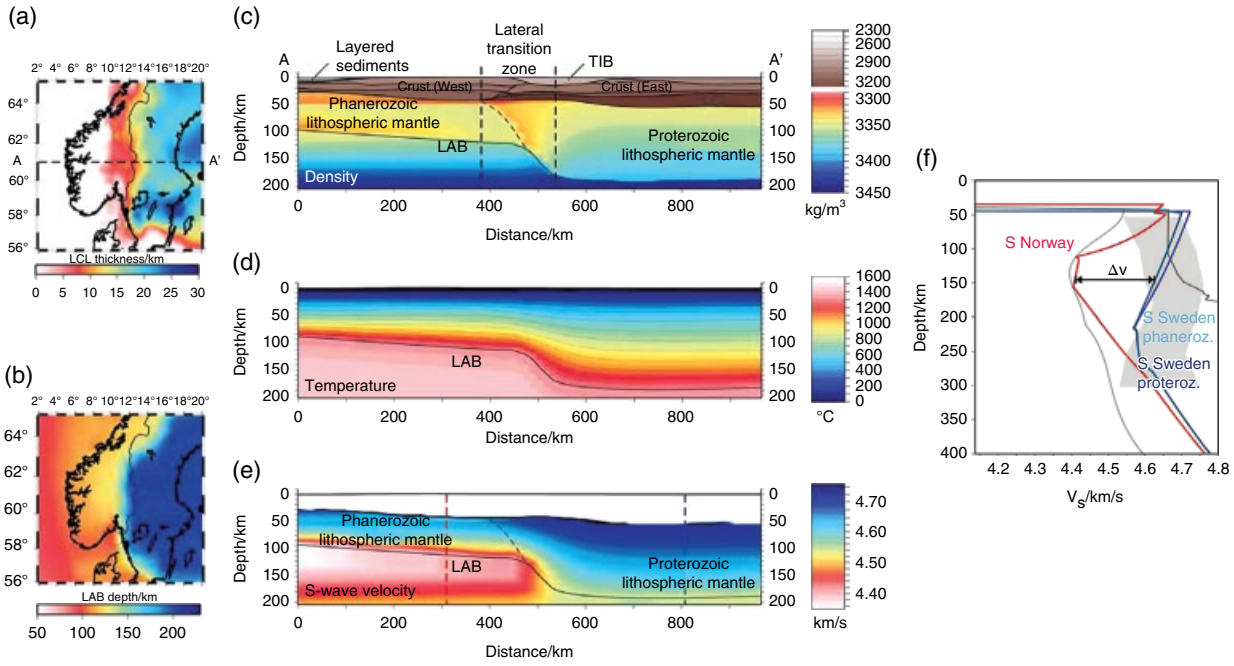

Figure 10.6 **(a)** Thickness of lower crustal layer (LCL). **(b)** Depth to thermal lithosphere–asthenosphere boundary (LAB). **(c)** Cross section at 61 °N showing the subsurface density distribution and general model structure (TIB, Transscandinavian Igneous Belt). **(d)** Temperature structure along cross section (c). **(e)** S-wave velocity along cross section (c) showing an overall velocity increase to the east. **(f)** Comparison of measured (*black lines*) and modeled (*red, blue*) velocities of southern Norway and southern Sweden. The *gray band* represents velocities from other Archean and Proterozoic cratons. After *Gradmann et al.* [2013].

confirmed that the topography in the Scandinavian orogen is isostatically compensated, in absence of a significant crustal root, by lateral changes in the lower crust and lithospheric mantle structure. They also showed that (i) a step-like increase in lithosphere thickness exists from southern Norway towards Sweden and (ii) a chemical change from fertile Phanerozoic mantle in southern Norway to a more depleted Proterozoic composition exists beneath southern Sweden (Figure 10.6). This lateral transition zone roughly separates Meso- to Neo-Proterozoic and Palaeo-Proterozoic tectonothermal domains, delineating the long-lived edge of the Baltic craton and the Fennoscandia domain. A somewhat similar methodology has been more recently introduced by *Kaban et al*. [2014] and *Tesauro et al*. [2014] and used to study the North American lithosphere.

10.5. THERMOCHEMICAL STRUCTURE FROM MULTI-OBSERVABLE PROBABILISTIC METHODS

The modeling approaches described in the previous section can provide useful first-order information on the thermochemical structure of the lithosphere provided enough information is available to the modeler. However, such methods are not well prepared to deal with one or more of the following problems:

1. Strong nonlinearity of the system. Traditional linearized inversions do not generally provide reliable estimates of the thermochemical structure of the Earth.
2. The temperature effect on geophysical observables is in most cases greater than the compositional effect; therefore the latter is significantly more difficult to isolate.
3. Nonuniqueness of the compositional field. Different compositions can fit equally well seismic and potential field observations (Figure 10.7).
4. Strong correlations between physical parameters and geophysical observables complicate the inversion procedure and their effects are poorly understood.
5. Trade-off between temperature and composition in wave speeds.
6. Uncertainties affecting the results are difficult to estimate.

Taking into account all these considerations, a robust characterisation of the 3D thermochemical structure of the upper mantle would require six basic ingredients:

• Representative and general a priori information on compositional space. Given that the problem of retrieving a single composition from geophysical information has

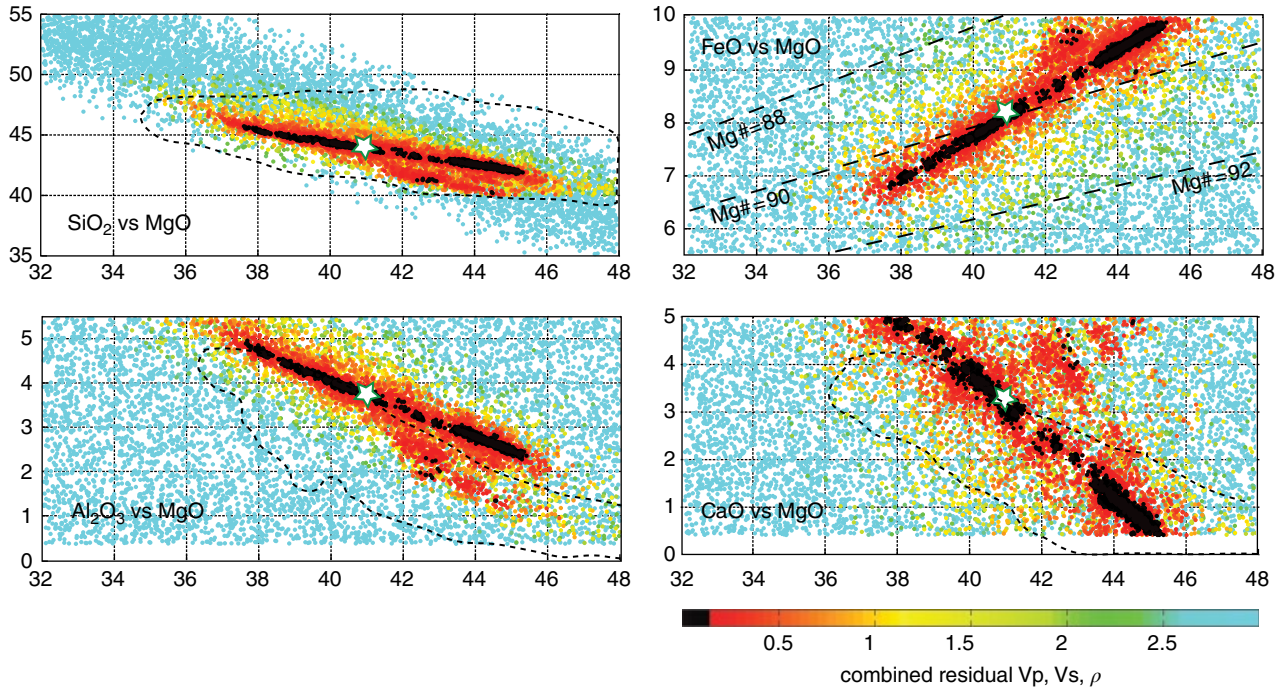

Figure 10.7 Monte Carlo search within the "peridotitic" compositional space of samples that fit a specific set of seismic velocities and bulk density (indicated by the *white star*). All *black samples* are identical, for all practical purposes, in terms of their physical properties and therefore a unique best solution is difficult (impossible?) to justify based on physical properties only. The *dashed envelopes* encircle > 95% of the natural samples shown in Figure 10.2. Provided that this database is representative of the natural variability in the lithospheric mantle, it can be used as prior information to minimize the number of possible solutions (e.g., *Afonso et al*. [2013a,b]).

no unique solution [*Afonso et al*., 2013a], the role of a priori information is critical. This prior information should be general enough to cover the entire spectrum of observed/expected bulk compositions in mantle peridotites, from fertile (or refertilized) lithospheric mantle to highly depleted harzburgites and dunites.

• Thermodynamic consistency between thermal and compositional parameters. This means that parameters such as bulk density, bulk modulus, or shear-wave velocity are not free to vary independently, but are linked together by the fundamental laws of thermodynamics; the only independent variables in the system are temperature, pressure, and composition. This guarantees that no violation of thermodynamic principles will occur during the modeling or inversion (something that is impossible when using assumed ratios such as ρ/Vs; e.g., see *Forte* [2007] and *Simmons et al*. [2010]).

• Internal consistency between observables and the thermochemical state of the mantle. This means that all calculated observables (e.g., dispersion curves, travel times, etc.) are only and ultimately dependent on temperature, pressure, and composition (the governing independent variables) while being linked together by robust and sound (typically nonlinear) physical theories. This guarantees that a local change in properties such as density or Vs, which may be required to improve the fitting of a particular observable, will be also reflected in all other observables in a consistent manner. It also implies that no linearity between observables needs to be assumed; each observable responds according to its own governing physical theory (e.g., sound propagation).

• The use of multiple observables, each sensitive to different aspects of the problem. This minimizes the range of acceptable models by increasing the number of constraining datasets. This requires that each observable has a different sensitivity to the main parameters (T, P, composition). This seemingly obvious requirement is crucial when the uncertainties in observations are considered. Every new observable carries uncertainties that are propagated to the final result. Therefore, if a new observable is added to the inversion, but its sensitivity is equal to or less than other previous observables, the net effect could be a degradation of the results.

• Representative estimation of uncertainties, preferably as full posterior probability density functions. This is critical when working with different datasets subject to different uncertainties (both in nature and magnitude). In this context, probabilistic methods provide a natural way to deal with both theoretical/methodological and observational uncertainties into the inversion problem. The final posterior distribution (i.e., result of the inversion) is in itself a measure of the uncertainties affecting the results.

• Generality and objectivity. This requirement ensures the inverse framework is applicable to a large number of scenarios (e.g., different tectonic settings, different terrestrial bodies) and to a multitude of data with the minimum (necessary) input of subjective information.

A number of recent efforts have focused on developing methods honoring these ingredients and capable of directly inverting geophysical, geochemical, and/or geodetic data sets for the fundamental thermodynamic variables inside the Earth, namely temperature, pressure, and composition [*Khan et al*., 2009, 2011; *Kuskov et al*., 2011, 2014; *Afonso et al*., 2013a,b, 2014]. One approach that holds great promise for obtaining reliable images of the temperature and compositional structure of the lithosphere and upper mantle is based on the joint inversion of multiple datasets within a probabilistic (Bayesian) framework. In the past 20 years, Bayesian methods applied to inverse problems have become standard and powerful tools in geophysics, and many review papers and textbooks are now available on the subject (cf. *Mosegaard* [1998], *Bosch* [1999], *Mosegaard and Tarantola* [1995], *Mosegaard and Sambridge* [2002], *Tarantola* [2005], *Idier* [2008], *Biegler et al*. [2011]). *Khan et al*. [2009, 2011] and *Afonso et al*. [2013a,b] provide detailed discussions on the advantages of probabilistic over traditional (nonprobabilistic) inversion methods when studying the thermochemical structure of the mantle. In addition, probabilistic methods can easily deal with multiscale parameterizations (multiple resolutions) needed to simultaneously invert datasets of different nature, and they allow to work with realistic (complex) Earth models. When combined with robust thermodynamic formalisms (e.g., see *Stixrude and Lithgow-Bertelloni* [2005] and *Ganguly et al*. [2009]) to solve the forward problems (i.e., prediction of observables), probabilistic methods offer the most general, and arguably the best, solution to invert for possible compositional structures within the upper mantle. On the downside, probabilistic inversion methods rely on long Markov Chain Monte Carlo (MCMC) simulations, in which the forward problems are solved typically on the order of 10^4 to 10^8 times, making them much more time-consuming and computationally expensive than traditional matrix-based methods.

In order to relate seismic structure to the actual/absolute physical state of the lithosphere and upper mantle using thermodynamic formalisms (i.e., absolute temperature, bulk composition, etc.), we need information on absolute rather than relative wave speeds. Thus, surface wave tomography seems to be more adequate to this end than teleseismic tomography. In this context, phase–velocity dispersion maps obtained from the combination of ambient noise tomography with teleseismic surface wave tomography constitute one of the best sources of information for retrieving absolute Vs values in the lithosphere and sublithospheric upper mantle (see Section 10.4.2). The recent extension of ambient noise techniques to

obtain long-period (up to 150 sec) dispersion maps [*Yang*, 2014] bypasses the need to complement short-period ambient noise dispersion data with teleseismic earthquake data and represents a potentially excellent source of absolute Vs values at lithospheric depths. However, surface wave data from fundamental mode observations are not sensitive to structure at depths below ~300 km and their lateral resolution is poorer than body wave data (in dense arrays). Although the inclusion of overtones can in principle increase the sensitivity of surface waves to deeper structure (e.g., see *van Heijst and Woodhouse* [1999], *Visser et al*. [2008], *Khan et al*. [2011], and *Schaeffer and Levedev* [2013]), the limited lateral resolution remains an issue in regional studies.

A number of authors have combined the individual strengths of surface wave and body wave teleseismic data to map the absolute velocity structure of the upper mantle (e.g., see *West et al*. [2004], *Rawlinson and Fishwick* [2011], and *Obrebski et al*. [2011]. Similarly, teleseismic tomography and surface wave tomography can be combined under a thermodynamically constrained probabilistic inversion scheme to obtain direct estimates of the temperature and compositional structure of the lithosphere and upper mantle. In this approach, Vp, Vs, and bulk density are linked through sound thermodynamic relationships, and therefore any Vs structure used to fit, for example, dispersion data has an equivalent and thermodynamically consistent Vp structure that can be used to solve the P-wave teleseismic problem (accounting for frequency-dependent attenuation). Given the time involved in computing teleseismic travel times in a 3D volume (a nonlinear problem), the implementation of grid-based eikonal solvers within probabilistic inversions is challenging. *Afonso et al*. [2014] have recently tackled this problem with a strategy that, albeit simple, provides reliable results. The authors do not solve the nonlinear problem at every step of the MCMC random walk, but only every *n* predefined steps instead. In between these *n* nonlinear solutions, travel-time residuals are computed by a simple integration of slowness along each fixed ray path. This locally linear approximation therefore assumes that the ray-path geometry is independent of the actual velocity structure. This is a reasonable approximation for teleseismic paths as long as the model does not change significantly between each nonlinear step. Moreover, by updating the paths every *n* steps as the inversion proceeds, the nonlinear behavior of the system is ultimately explicitly considered. The choice of *n* depends on the region under study, and it can be chosen based on preliminary tests [*Afonso et al*., 2014]. One difficulty associated with this approach is the assumption of a spherically symmetric Earth outside the target volume. Several studies have shown that heterogeneities in the lower mantle and transition zone can affect the amplitude of the velocity anomalies in standard regional tomography methods (e.g., see *Masson and Trampert* [1997], *Bijwaard et al*. [1998], and *Zhao et al*. [2013]). However, the general pattern of anomalies is not significantly affected [*Zhao et al*., 2013]. Since the method in *Afonso et al*. [2014] does not rely on recovered amplitudes, it is unclear whether the improvement that would be gained by considering a global velocity model outside the target volume justifies the significant increase in computational time. Further tests are needed to evaluate this possibility.

An important difficulty that needs to be emphasized when estimating temperature and composition in the mantle is the fact that no unique composition can be generally found; an entire population of compositions can generally fit the data equally well. This is neither related to the primitive uncertainties associated with the datasets nor related to the theoretical uncertainties affecting forward solvers. It is an intrinsic feature displayed by mantle rocks/minerals [*Afonso et al*., 2013a]. This is illustrated in Figure 10.7, which shows the results of an extensive parameter space search using the Neighbourhood Algorithm of *Sambridge* [1999]. The search is guided by a simple (L1) misfit function of the form

$$\text{misfit} = \left|\rho^p - \rho^o\right| + \left|Vp^p - Vp^o\right| + \left|Vs^p - Vs^o\right|, \qquad (10.1)$$

where the superscripts ^{p} and ^{o} refer to "predicted/theoretical" and "observed/true," respectively, and $|\cdots|$ brackets indicate absolute values. Predicted values of bulk density and sound velocities are computed at T = 900°C, P = 1.2 GPa by energy minimization [*Connolly*, 2009] following the thermodynamic formalism of *Stixrude and Lithgow-Bertelloni* [2005] and the thermodynamic database of *Xu et al*. [2008]. For all practical purposes, all samples in black are characterized by identical bulk ρ, Vp, and Vs, and therefore they explain the original data equally well. Note that this example represents the best possible scenario, where we have true values of the actual physical parameters. In a real case scenario, however, we would have to invert real data (e.g., gravity anomalies, travel times, etc.) subject to observational uncertainties, which would further expand the space of valid solutions.

The example above highlights the critical role of a priori information on the compositional space. Two common approaches to reducing the population of valid solutions are either assigning tighter bounds to the compositional space or working with a linear combination of basaltic and harzburgitic/dunitic end-member components to represent the fertile-depleted trend of peridotites. The first option usually uses local xenolith information (e.g., see *James et al*. [2004], *Roy et al*. [2005], and *Fullea et al*. [2010]) or empirical correlations between the age of the overlying crust and the composition of the lithospheric mantle (e.g., see *Carballo et al*. [2015]). While

practical and convenient, this approach also represents a highly subjective option that cannot be used to explore the compositional heterogeneity of the lithospheric mantle. The second option constitutes a more general approach, especially in large-scale studies (e.g., see *Khan et al*. [2011] and *Ritsema et al*. [2009]), but it still leaves a large portion of the naturally occurring compositional variability unrepresented (Figure 10.3). One way of including a priori compositional information into multi-observable inversions without compromising generality and representativeness has been presented in *Afonso et al*. [2013a]. The approach is based on a large database of natural and well-studied mantle samples (from xenoliths, abyssal peridotites, ophiolites, etc.) and on robust correlations between major oxides. This database is used to derive multidimensional probability density functions in the "peridotitic" compositional space that describe the natural variability observed in samples from many different tectonic settings (Figure 10.3). However, other minor mantle lithologies such as eclogites and pyroxenites were not included explicitly as part of the a priori PDFs used in *Afonso et al*. [2013a], and therefore its application is strictly valid if the assumption of an upper mantle dominated by peridotite holds true. If large amounts of basaltic or eclogitic material are present as mechanically and chemically independent lithologies (e.g., see *Xu et al*. [2008], *Khan et al*. [2011], and *Ritsema et al*. [2009]), the above approach should be extended to include these lithologies. However, more work towards subjecting the mixture hypothesis to rigorous tests (using multiple geophysical observables), as well as to geochemical/geodynamic arguments, is still needed.

10.6. THE PROMISING FUTURE

The last 20 years have witnessed an outstanding increase in both the amount and quality of geophysical data pertinent to the lithosphere and upper mantle. The data and images obtained with dense broadband arrays such as USArray, ChinaArray, and IberArray have clearly demonstrated their value and effectiveness in characterizing the fine-scale structure of the lithosphere and upper mantle. Although difficult to predict, the deployment of such arrays in other regions of the world surely will become more common in the near future. Likewise, satellite missions are providing cost-effective global databases of the topography, magnetic, and gravity fields with ever-increasing resolution and accuracy. The gradiometric and magnetic measurements provided by the ESA GOCE and Swarm missions represent a recent example of the utility and potential of global satellite data in studying the lithosphere [e.g. *Bouman et al.*, 2013; *Fullea et al.*, 2015]. Dense magnetotelluric arrays, often coincident with seismic broadband arrays (e.g., USArray, IberArray) are also becoming more popular (e.g., see *Meqbel et al.* [2014], *Dong et al.* [2011], and Stolz [2013]), and this is a trend likely to continue.

Taking full advantage of all these datasets (and others not mentioned, e.g., GPS, A-DInSAR surface motion) requires methods capable of inverting/modeling multiple observables, with different resolutions and sensitivities to different features of the Earth's interior. We have argued in this chapter that probabilistic methods offer a viable, and perhaps the best, approach to inverting multiple datasets for the physical state of the lithosphere and upper mantle. However, multi-observable probabilistic inversions still is a relatively understudied field, and a number of conceptual and technical difficulties remain to be addressed and circumvented. For instance, a realistic and formal treatment of both observational and theoretical uncertainties is challenging, yet critical (e.g., *Afonso et al*. [2013a,b], *Fournier et al*. [2013], and *Rawlinson et al*. [2014]). Also, more efficient and robust parallel MCMC algorithms to jointly invert massive multiple datasets will be needed. In this context, working with significantly different forward problems (different resolutions and sensitivities) that cannot be related to each other using a unique physical theory can create conflict between predictions that may be difficult to reconcile. In other words, while one observable guides the solution towards one set of model parameters, another observable points towards a different set. Although this can create an internal conflict that poses a serious challenge to the modeler as well as to common MCMC optimization algorithms, the fact that the inversion gives conflicting solutions does not necessarily mean that the observables have an intrinsic conflicting nature. At least in some cases, this conflicting behavior is rooted in the parameterization/design of our forward models. Therefore, the detection of such inconsistencies can inform the user about aspects of the model that are not well understood or dealt with, which in itself represents a gain of information. Regardless of whether the inconsistency lies in the design of the forward problem (or model) or in the nature of the observables, the problem is typically exacerbated when single-objective MCMC algorithms are used. Strictly, multiobservable inversion is a multiobjective or vector optimization problem (cf. *Marler and Arora* [2004]) and standard scalarization (or weighted-sum) single-objective approaches, typically used in geophysics, are not guaranteed to offer a good sampling of the complete pareto-optimal set (e.g., see *Das and Dennis* [1998] and *Marler and Arora* [2004]). The latter is an important ingredient of multiobjective optimization that provides critical and systematic information on the trade-offs between model parameters and the multiobjective functions used in the inversion. Moreover, the selection of weights to form the single-objective (or misfit) function is typically problem-dependent and involves a great deal of

calibration and subjective input by the modeler. This can make the inversion process inefficient. However, an exploration of full multiobjective methods in the context of multiobservable inversions for the physical state of the Earth is not only nonexistent, but also beyond the scope of the present paper. We leave this issue for future work.

Working under a scheme that allows taking full advantage of complex forward problems is also important to move towards a more holistic approach to imaging the Earth's interior. Clearly, the generation of thermophysical models that are simultaneously constrained by multiple geophysical and geodynamic observables would bring a qualitative leap in our understanding of the nature and evolution of the lithosphere, its interaction with the sublithospheric mantle, and the driving forces responsible for plate motion. Several approaches have been proposed for solving the joint geodynamic-gravity-seismic inversion/modeling problem; all of them are intended for low-resolution, large-scale models (e.g., see *Forte* [2007], *Forte* [2000] *Simmons et al*. [2006, 2010], and *Cammarano et al*. [2011]). One of the most popular and advanced approaches is that of *Simmons et al*. [2010], in which shear and compressional wave velocities are linked to bulk density through empirical mineral-physics parameters. In contrast to other similar approaches, *Simmons et al*. [2010] perform a real inversion of seismic data. However, this method still relies on two somewhat restrictive assumptions: (i) All responses of the system are assumed to be linear and (ii) temperature and compositional signatures are decoupled during the inversion. Future studies coupling consistently the dynamic behavior of the mantle with multiple surface observations, honoring the nonlinear and thermodynamic consistency of the system, will undoubtedly shed critical information about the internal workings of the Earth, particularly on the complex interaction between plates and the underlying convecting mantle. Some preliminary steps have been recently taken [*Afonso et al*., 2014], demonstrating the feasibility and potential of such inversions.

Similarly, the migration from approaches based on ray theory to finite frequency and full waveform approaches seems to be an obvious next step in multiobservable inversions. Both tomography methods hold great potential to improve on the quality of thermochemical and seismic images of the upper mantle, particularly at regional and continental scales (e.g., see *Chevrot and Zhao* [2007], Nolet [2008], *Liu and Gu* [2012], *Fitchner et al*. [2013], and *Yuan et al*. [2014]). Likewise, inclusion of global information into the computation of teleseismic travel times (to explicitly account for the effect of deep anomalies) can be of benefit [*Zhao et al*., 2013]. However, since the use of more traditional ray-based approaches in multiobservable probabilistic inversion methods still is in its initial stages of development [*Afonso et al*., 2014], it is unclear at the moment to what extent results will be improved by implementing the above approaches or whether the additional benefits will outweigh the extra computational cost. Based on current trends, these issues are expected to be addressed in the next decade.

10.7. FINAL REMARKS

Integrated modeling and joint inversions for the structure of the lithosphere and upper mantle are becoming increasingly popular, partly because of the advances reviewed in this chapter. The recognition that working with complementary datasets provides a substantially more instructive view of the Earth is not new, but surprisingly practical implementations of such joint or multiobservable approaches are still far less common than single-data approaches. Working with multiple datasets demands a multidisciplinary framework and a diverse set of skills that in most cases go beyond geophysics, well into geochemistry, thermodynamics, and petrology. The more we learn about our planet, the more we recognize the importance of understanding it as a complex, dynamic physical entity rather than a static object described by stiff physical parameters such as mean density, seismic velocity, coefficients of thermal expansion, and so on. And when we pay attention to these complexities, to the great variety of links between physical and chemical processes within the Earth, we realize the importance of the connections between traditional disciplines. Unfortunately, traditional geophysics university programs tend to underestimate these connections, something that we believe will change in the next decade or so. This book is testament to the increasing interest in the solid Earth community regarding such integrated studies.

ACKNOWLEDGMENTS

Much of the material presented here is the result of many discussions with many colleagues over the years. We are particularly indebted to N. Rawlinson, Y. Yang, A. G. Jones, J. A. D. Connolly, W. Griffin, S. O'Reilly, B. Kennett, H. Yuan, S. Karato, U. Faul, S. Zlotnik, M. Fernandez, D. Schutt, S. Lebedev, H. Zeyen, M. Sambridge, A. Khan, S. Thiel, G. Heinson, and M. Qashqai. We thank S. I. Karato and F. Deschamps for their detailed and most valuable comments on an earlier version of this chapter. The work of JCA has been supported by an Australian Research Council Discovery Grant (DP120102372). JF was supported by the JAE-DOC programme (CSIC-Spain) co-founded by ESF, as well as by Spanish Ministry of Economy and Competitiveness grant CGL2012-37222, and funded by the People Programme (Marie Curie Actions) of the European Union's H2020-MSCA-IF-2014 programme under REA grant agreement n° 657357. This is contribution 619 from the ARC Centre of Excellence for Core to Crust Fluid Systems (http://www.ccfs.mq.

edu.au) and 1006 in the GEMOC Key Centre (http://www.gemoc.mq.edu.au).

REFERENCES

Afonso, J. C., and D. Schutt (2012), The effects of polybaric partial melting on the density and seismic velocities of mantle restites, *Lithos*, *134–135*, 289–303.

Afonso, J. C., M. Fernàndez, G. Ranalli, W. L. Griffin, and J. A. D. Connolly (2008a), Integrated geophysical–petrological modelling of the lithospheric-sublithospheric upper mantle: methodology and applications. *Geochem. Geophys. Geosyst. 9*, Q05008, doi:10.1029/2007GC001834.

Afonso, J. C., S. Zlotnik., and M. Fernandez (2008b), The effects of compositional and rheological stratifications on small-scale convection under the oceans: implications for the thickness of oceanic lithosphere and seafloor flattening, *Geophys. Res. Lett.*, *35*, doi:10.1029/2008GL035419.

Afonso, J. C., G. Ranalli, M. Fernandez, W. L. Griffin, S. Y. O'Reilly, and U. Faul (2010), On the Vp/Vs–Mg# correlation in mantle peridotites: Implications for the identification of thermal and compositional anomalies in the upper mantle. *Earth Planet. Sci. Lett.*, *289*, 606–618.

Afonso, J. C., J. Fullea, W. L. Griffin, Y. Yang, A. G. Jones, J. A. D. Connolly, and S. Y. O'Reilly (2013a), 3-D multi-observable probabilistic inversion for the compositional and thermal structure of the lithosphere and upper mantle. I: A priori petrological information and geophysical observables, *J. Geophys. Res. Solid Earth*, *118*, 25862617, doi:10.1002/jgrb.50124.

Afonso, J. C., J. Fullea, Y. Yang, J. A. D. Connolly, and A. G. Jones (2013b), 3-D multi-observable probabilistic inversion for the compositional and thermal structure of the lithosphere and upper mantle. II: General methodology and resolution analysis, *J. Geophys. Res. Solid Earth*, *118*, 16501676, doi:10.1002/jgrb.50123.

Afonso, J.C., Rawlinson, N., Yang, Y., Schutt, D., Jones, A., Fullea, J. (2014), Multi-observable probabilistic tomography reveals the thermochemical structure of Central-Western US. AGU Fall Meeting, Abstract S51B-4467.

Agius, M. R., and Lebedev, S. (2013), Tibetan and Indian lithospheres in the upper mantle beneath Tibet: Evidence from broadband surface-wave dispersion. *Geochem. Geophys. Geosyst.*, *14*, 42604281, doi:10.1002/ggge.20274.

Aizawa, Y., Barnhoorn, A., Faul, U.H., Fitz Gerald, J.D., Jackson, I., Kovcs, I. (2008) Seismic properties of Anita Bay Dunite: An exploratory study of the influence of water. *J. Petrol.*, *49*, 841–855.

Aki, K., and Lee, W. H. K. (1976), Determination of three-dimensional velocity anomalies under a seismic array using first P-arrival times from local earthquakes, 1, homogeneous initial model. *J. Geophys. Res.*, *81*, 4381–4399.

Alasoniati-Tasarova, S., J. C. Afonso, M. Bielik, H-J. Goetze, and J. Hok. (2009), The lithospheric structure of the Western Carpathian–Pannonian Basin region based on the CELEBRATION 2000 seismic experiment and gravity modelling. *Tectonophysics*, *475*, 454–469.

Ammon, C. J., G. E. Randall, and G. Zandt (1990), On the non-uniqueness of receiver function inversions, *J. Geophys. Res.*, *95*(B10), 1530315318, doi:10.1029/JB095iB10p15303.

Anderson, D. (1989), *Theory of the Earth*, Blackwell Scientific Publications, Oxford, UK.

Anderson, O. L., and D.G. Isaak (1995), Elastic constants of mantle minerals at high temperature, in *Mineral Physics and Crystallography: A Handbook of Physical Constants*, J. Ahrens, ed., AGU reference shelf 2, Washington, D.C.

Artemieva, I. M. (2009), The continental lithosphere: Reconciling thermal, seismic, and petrologic data, *Lithos 109*, 23–46.

Artemieva, I.M. (2011), *The Lithosphere: An Interdisciplinary Approach*, Cambridge University Press, Cambridge, UK.

Aubaud, C., E. H. Hauri, and M. M. Hirschmann (2004), Hydrogen partition coefficients between nominally anhydrous minerals and basaltic melts, *Geophys. Res. Lett.*, *31*, L20611, doi:10.1029/2004GL021341.

Aubaud, C., M. M. Hirschmann, A. C. Withers, and R. L. Hervig (2008), Hydrogen partitioning between melt, clinopyroxene, and garnet at 3 GPa in a hydrous MORB with 6 wt.% H_2O, *Contrib. Min. Petrol.*, *156*, 607–625.

Bailey, R. C. (1970), Inversion of the geomagnetic induction problem, *Proc. R. Soc. London*, *315*, 185–194.

Becker, T. W. (2012), On recent seismic tomography for the western United States, *Geochem. Geophys. Geosyst*., *13*, Q01W10, doi:10.1029/2011GC003977.

Bedrosian, P. A. (2007), MT+ integrating magnetotellurics to determine earth structure, physical state, and processes, *Surv. Geophys.*, *28*, 2–3, 121–167.

Bedrosian, P. A., N. Maercklin, U. Weckmann, Y. Bartov, T. Ryberg, and O. Ritter (2007), Lithology-derived structure classification from the joint interpretation of magnetotelluric and seismic models, *Geophys. J. Int.*, *170*, 737–748.

Bennington, N. L., H. Zhang, C. H. Thurber, and P. A. Bedrosian (2015), Joint inversion of seismic and magnetotelluric data in the Parkfield region of California using the normalized cross-gradient constraint, *Pure Appl. Geophys*., *172*, 1033–1052.

Biegler, L., et al. (eds.) (2011), *Large-Scale Inverse Problems and Quantification of Uncertainty*, John Wiley & Sons, UK.

Bijwaard H., W. Spakman, and E. R. Engdahl (1998), Closing the gap between regional and global traveltime tomography, *J. Geophy. Res.*, *103*, 3005530078.

Bodinier, J.-L., C. J. Garrido, I. Chanefo, O. Bruguier, and Gervilla, F. (2008), Origin of pyroxeniteperidotiteveined mantle by refertilization reactions: Evidence from the ronda peridotite (Southern Spain), *J. Petrol.*, *49*, 999–1025.

Bodinier, J.-L., and M. Godard (2003), Orogenic, ophiolitic, and abyssal peridotites, in *The Mantle and Core*, R. W. Carlson, ed., Vol. *2*, *Treatise on Geochemistry*, H. D. Holland, and K. K Turkeian, eds., Elsevier-Pergamon, Oxford.

Bolfan-Casanova, N., H. Keppler, and D.C. Rubie (2000), Water partitioning between nominally anhydrous minerals in the $MgO–SiO_2–H_2O$ system up to 24 GPa: Implications for the distribution of water in the Earth's mantle, *Earth Planet. Sci. Lett.*, *182*, 209–221.

Bosch, M. (1999), Lithologic tomography: From plural geophysical data to lithology estimation, *J. Geophys. Res.*, *104*(B1), 749766, doi:10.1029/1998JB900014.

Bowin, C. (2000), Mass anomaly structure of the Earth, *Rev. Geophys.*, *38*(3), 355–387.

Burov, E. B. (2011), Rheology and strength of the lithosphere, *Marine Petrol. Geol.*, *28*, 1402–1443.

Cammarano F., P. Tackley, and L. Boschi (2011), Seismic, petrological and geodynamical constraints on thermal and compositional structure of the upper mantle: Global thermochemical models, *Geophys. J. Int.*, *187*, 1301–1318.

Carballo, A., M. Fernandez, M. Torne, I. Jimnez-Munt, and A. Villaseor (2015), Thermal and petrophysical characterization of the lithospheric mantle along the northeastern Iberia geo-transect, *Gondwana Res*., http://dx.doi.org/10.1016/j.gr.2013.12.012.

Carlson, R. W., D. G. Pearson, and D. E. James (2005), Physical, chemical, and chronological characteristics of continental mantle. *Rev. Geophys*., *43*, RG1001, 1–24.

Chappell, A. R., and N. J. Kusznir (2008), Three-dimensional gravity inversion for Moho depth at rifted continental margins incorporating a lithosphere thermal gravity anomaly correction, *Geophys. J. Int*., *174*(1) (2008), 113.

Chen, C.-W., S. Rondenay, R. L. Evans, and D. B. Snyder (2009), Geophysical detection of relict metasomatism from an Archean (3.5 Ga) subduction zone, *Science*, *20*, 326, 1089–1109.

Chevrot, S., and L. Zhao (2007), Multiscale finite-frequency Rayleigh wave tomography of the Kaapvaal craton. *Geophys. J. Int.*, *169*, 201–215.

Connolly, J. A. D. (2009), The geodynamic equation of state: What and how, *Geochem. Geophys. Geosyst.*, *10*, Q10014, doi:10.1029/2009GC002540.

Conrad, C. P., and C. Lithgow-Bertelloni (2006), Influence of continental roots and asthenosphere on platemantle coupling, *Geophys. Res. Lett.*, *33*, doi:10.1029/2005GL025621.

Constable, S. C., and R. L. Parker, and C. G. Constable (1987), Occam's inversion: A practical algorithm for generating smooth models from electromagnetic sounding data, *Geophysics*, *52*, 289–300.

Dai, L., and S. I. Karato (2009), Electrical conductivity of orthopyroxene: Implications for the water content of the asthenosphere, *Proc. Japan Acad., Ser. B, Phys. Biol. Sci*., *85*, 466.

Dai, L., and S.-I. Karato (2014), High and highly anisotropic electrical conductivity of the asthenosphere due to hydrogen diffusion in olivine, *Earth Planet. Sci. Lett.*, *408*, 79–86.

Das, I., and J. E. Dennis (1998), Normal-boundary intersection: A new method for generating the Pareto surface in nonlinear multicriteria optimization problems, *SIAM J. Optim*, *8*, 631657.

Deschamps, F., R. Snieder, and J. Trampert (2001), The relative density-to-shear velocity scaling in the uppermost mantle. *Phys. Earth Planet. Inter*., *124*(3), 193–212.

Doin, M. P., L. Fleitout, and D. P. McKenzie (1996), Geoid anomalies and the structure of continental and oceanic lithospheres, *J. Geophys. Res.*, *101*, 16119–16135.

Dong, S., T. Li, R. Gao, H. Hou, Y. Li, S. Zhang, and M. Liu (2011), A multidisciplinary earth science research program in China, Eos, *Transactions American Geophysical Union*, *92*(38), 313–314.

Downes, H. (2007), Origin and significance of spinel and garnet pyroxenites in the shallow lithospheric mantle: Ultramafic massifs in orogenic belts in Western Europe and NW Africa. *Lithos*, *99*, 1–24.

Eaton, D. W., F. Darbyshire, R. L. Evans, H. Grutter, A. G. Jones, and X. Yuan (2009), The elusive lithosphere–asthenosphere boundary (LAB) beneath cratons, *Lithos*, *109*, 1–22.

Ebbing, J., C. Braitenberg, and H.-J. Gtze (2006), The lithospheric density structure of the Eastern Alps, *Tectonophysics*, *414*, 145–155. doi:10.1016/j.tecto.2005.10.015.

Eberhart-Phillips, D. (1990), Three-dimensional P and S velocity structure in the Coalinga Region, California. *J. Geophys. Res.*, *95*, 15343–15363.

Evans, J. R., and Achauer, U. (1993), Teleseismic velocity tomography using the ACH method: Theory and application to continental-scale studies, in *Seismic Tomography*, H. M. Iyer and K. Hirahara, eds., Chapman & Hall, London, pp. 319–360.

Evans, R. L., et al. (2011), Electrical lithosphere beneath the Kaapvaal craton, southern Africa, *J. Geophys. Res.*, *116*, B04105, doi:10.1029/2010JB007883.

Evans, R. L., and G. Hirth, K. Baba, D. Forsyth, A. Chave, and R. Mackie (2005), Geophysical evidence from the MELT area for compositional controls on oceanic plates, *Nature*, *437*, 249–252.

Fernandez, M., M. Torne, D. Garcia-Castellanos, J. Verges, W. Wheeler, and R. Karpuz (2004), Deep structure of the Vring Margin: The transition from a continental shield to a young oceanic lithosphere, *Earth Planet. Sci. Lett.*, *221*, 131–144.

Fernàndez, M., J. C. Afonso, and G. Ranalli (2010), The deep lithospheric structure of the Namibian volcanic margin, *Tectonophysics*, *481*, 68–81.

Ferot, A. and Bolfan-Casanova, N. (2012), Water storage capacity in olivine and pyroxene to 14GPa: Implications for the water content of the Earth's upper mantle and nature of seismic discontinuities, *Earth Planet. Sci. Lett.*, *349*, 218–230.

Fichtner A., J. Trampert, P. Cupillard, E. Saygin, T. Taymaz, Y. Capdeville, and A. Villasenor (2013), Multiscale full waveform inversion. *Geophys. J. Int.*, *194*, 534–556.

Fischer, K. M., H. A. Ford, D. L. Abt, and C. A. Rychert (2010), The lithosphere-asthenosphere boundary, *Annu. Rev. Earth Planet. Sci*., *38*, 551–575.

Fischer, K. M., H. A. Ford, D. L. Abt, and C. A. Rychert (2013), The lithosphere–asthenosphere boundary, *Annu. Rev. Earth Planet. Sci.*, *38*, 551–575.

Fishwick, S., M. Heintz, B. L. N. Kennett, A. Reading, and Y. Yoshizawa (2008), Steps in lithospheric thickness within eastern Australia, evidence from surface wave tomography. *Tectonics*, *27*, doi:10.1029/2007TC002116.

Forte, A. M. (2000), Seismic–geodynamic constraints on mantle flow: Implications for layered convection, mantle viscosity, and seismic anisotropy in the deep mantle, in *Earth's Deep Interior: Mineral Physics From the Atomic to the Global Scale, Geophysics Monograph Series 117*, by S. I. Karato et al., eds., AGU, Washington, DC, p. 336.

Forte, A. M. (2007), Constraints on seismic models from other diciplines—Implication for mantle dynamics and composition, in *Treatise of Geophysics*, Vol. *1*, B. Romanowicz and A. M. Dziewonski, eds., Elsevier, Oxford, pp. 805–854.

Forte, A. M., and J. X. Mitrovica (2001), Deep-mantle high-viscosity flow and thermochemical structure inferred from seismic and geodynamic data, *Nature*, *410* (6832), 1049–1056.

Foulger, G., et al. (2013), Caveats on tomographic images, *Terra Nova*, *25*, 259–281.

Fournier, A., et al. (2013), Assessing uncertainty in geophysical problems—Introduction, *Adv. Geophys.*, *78*, 3, WB1–WB2.

Fullea, J., J. Fernandez, H. Zeyen, and J. Vergs (2007), A rapid method to map the crustal and lithospheric thickness using elevation, geoid anomaly and thermal analysis. Application to the Gibraltar Arc System, Atlas Mountains and adjacent zones, *Tectonophysics*, *430*, 97–117.

Fullea, J., M. Fernandez, and H. Zeyen (2008), FA2BOUG-a FORTRAN 90 code to compute Bouguer gravity anomalies from gridded free air anomalies: Application to the Atlantic–Mediterranean transition zone, *Comput. Geosci.*, *34*, 1665–1681, doi:10.1016/j.cageo.2008.02.018.

Fullea, J., J. C. Afonso, J. A. D. Connolly, M. Fernàndez, D. Garcia-Castellanos, and H. Zeyen (2009), LitMod3D: An interactive 3-D software to model the thermal, compositional, density, seismological, and rheological structure of the lithosphere and sublithosheric upper mantle. *Geochem. Geophys. Geosyst.*, *10*, Q08019, doi:10.1029/2009GC002391.

Fullea, J., M. Fernàndez, J. C. Afonso, J. Vergés, and H. Zeyen (2010), The structure and evolution of the lithosphere–asthenosphere boundary beneath the Atlantic–Mediterranean transition region. *Lithos*, *120*, 74–95.

Fullea, J., M. R. Muller, and A. G. Jones (2011), Electrical conductivity of continental lithospheric mantle from integrated geophysical and petrological modeling: Application to the Kaapvaal Craton and Rehoboth Terrane, southern Africa, *J. Geophys. Res.*, *116*, B10202, doi:10.1029/2011JB008544.

Fullea, J., J. Rodríguez-González, M. Charco, Z. Martinec, A. Negredo, and A. Villaseñor (2015), Perturbing effects of sub-lithospheric mass anomalies in GOCE gravity gradient and other gravity data modelling: Application to the Atlantic–Mediterranean transition zone, *Int. J. App. Earth Obs. Geoinf.*, *35*, 54–69.

Furlong, K. P., andD. S. Chapman (2013), Heat flow, heat generation, and the thermal state of the lithosphere, *Ann. Rev. Earth Planet. Sci.*, *41*, 385–410.

Fujii, I., and A. Schultz (2002), The 3D electromagnetic response of the Earth to ring current and auroral oval excitation, *Geophys. J. Int.*, *151*, 689–709.

Gallardo, L. A., and M. A. Meju (2007), Joint two-dimensional cross-gradient imaging of magnetotelluric and seismic traveltime data for structural and lithological classification, *Geophys. J. Int.*, *169*, 1261–1272.

Ganguly, J., A. M. Freed, and S. K. Saxena (2009), Density profiles of oceanic slabs and surrounding mantle: Integrated thermodynamic and thermal modeling, and implications for the fate of slabs at the 660 km discontinuity, *Phys. Earth Planet. Int.*, *172*, 257–267.

Gatzemeier, A., and M. Moorkamp (2005), 3D modelling of electrical anisotropy from electromagnetic array data: Hypothesis testing for different upper mantle conduction mechanisms, *Phys. Earth Planet. Int.*, *149*, 225–242.

Gatzemeier, A., and A. Tommasi (2006), Flow and electrical anisotropy in the upper mantle: Finite-element models constraints on the effects of olivine crystal preferred orientation and microstructure, *Phys. Earth Planet. Int.*, *158*, 92–106.

Gradmann, S., J. Ebbing, and J. Fullea (2013), Integrated geophysical modelling of a lateral transition zone in the lithospheric mantle under Norway and Sweden, *Geophys. J. Int.*, *194*, 1359–1374.

Grand, S. P. (1994), Mantle shear structure beneath the Americas and surroundings oceans, *J. Geophys. Res.*, *99*, 11591–11621.

Grant, K., J. Ingrin, J. P. Lorand, and P. Dumas (2007), Water partitioning between mantle minerals from peridotite xenoliths, *Contributions to Mineralogy and Petrology*, *154* (1), 15–34.

Granet, M., M. Wilson, and U. Achauer (1995), Imaging a mantle plume beneath the French Massif Central, *Earth Planet. Sci. Lett.*, *136*, 281–296.

Green, D. H., and T. J. Fallon (1998), Pyrolite: A Ringwood concept and its current expression, In *The Earth's Mantle edited by* I. Jackson, Cambridge University Press, pp. 311–378.

Green, D. H., W. O. Hibberson, I. Kovács, and A. Rosenthal (2010), Water and its influence on the lithosphere-asthenosphere boundary, *Nature*, *467* (7314), 448–451.

Griffin, W. L., S. Y. O'Reilly, and C. G. Ryan (1999), The composition and origin of sub-continental lithospheric mantle. In: Fei, Y. et al., (eds.), Mantle petrology: Field observations and high-pressure experimentation: A tribute to Francis R. (Joe) Boyd, Vol. 6, The Geochemical Society Houston, pp. 13–45.

Griffin, W. L., and S. Y. O'Reilly (2007), Cratonic lithospheric mantle: Is anything subducted? *Episodes*, *30*(1), 43–53.

Griffin, W. L., S. O'Reilly, J. C. Afonso, and G. Begg (2009), The composition and evolution of lithospheric mantle: A Re-evaluation and its tectonic implications, *J. Petrol.*, *50*(7), 1185–1204.

Hager, B. H. (1984), Subducted slabs and the geoid: Constraints on mantle rheology and flow, *J. Geophys. Res.*, *89*(B7), 60036015, doi:10.1029/JB089iB07p06003.

Hager, B. H., and Richards, M. A. (1989), Long-wavelength variations in Earth's geoid: Physical models and dynamical implications, *Phil. Trans. R. Soc. London*, *Math. Phys. Eng. Sci.*, *328*, 309–327.

Hasterok, D., and D. S. Chapman (2007), Continental thermal isostasy: 1. Methods and sensitivity, *J. Geophys. Res.*, *112*, B06414, doi:10.1029/2006JB004663.

Hasterok, D., and D. S. Chapman (2011), Heat production and geotherms for the continental lithosphere, *Earth Planet. Sci. Lett.*, *307*, 59–70, doi:10.1016/j.epsl.2011.04.034.

Heinson, G. (1999), Electromagnetic studies of the lithosphere and asthenosphere, *Surv. Geophys.*, *20*, 229–255.

Herzberg, C. (2004), Geodynamic information in peridotite petrology, *J. Petrol.*, *45*, 2507–2530.

Herzberg, C., and M. J. O'Hara (2002) Plume-associated ultramafic magmas of Phanerozoic age, *J. Petrol.*, *43*, 18571883.

Hirose, K., and T. Kawamoto (1995), Hydrous partial melting of lherzolite at 1 GPa: The effect of H_2O on the genesis of basaltic magmas, *Earth Planet. Sci. Lett.*, *133*, 463473.

Hirschmann, M. M. (2006), Water, melting, and the deep Earth's H_2O cycle, *Annu. Rev. Earth Planet. Sci.*, *34*, 629653.

Hirth, G., and D. L. Kohlstedt (1996), Water in the oceanic upper mantle: Implications for rheology, melt extraction and the evolution of the lithosphere, *Earth Planet. Sci. Lett.*, *144*, 93–108.

Hofmann, A. W. (1997), Mantle geochemistry: The message from oceanic volcanism, *Nature*, *385*, 219–229, doi:10.1038/385219a0.

Holland, T. J. B., and R. Powell (2011), An improved and extended internally consistent thermodynamic dataset for phases of petrological interest, involving a new equation of state for solids, *J. Metamorphic Geolo.*, *29*: 333383. doi: 10.1111/j.1525-1314.2010.00923.x

Idier, J. (2008), *Bayesian Approach to Inverse Problems*, John Wiley & Sons, UK.

Isacks, B. L., J. Oliver, and L. R. Sykes (1968), Seismology and the new global tectonics, *J. Geophys. Res.*, *73*, 5855–5899.

Jacob, D. E (2004), Nature and origin of eclogite xenoliths, *Lithos*, *77*, 295–316.

James, D. E., F. R. Boyd, D. Schutt, D. R. Bell, and R. W. Carlson (2004), Xenolith constraints on seismic velocities in the upper mantle beneath southern Africa, *Geochem. Geophysics. Geosys*., *5*(1), Q01002.

Jaupart, C., and J-C. Mareschal (2011), *Heat Generation and Transport in the Earth*, Cambridge University Press, Cambridge, UK.

Jiménez-Munt, I., M. Fernández, J. Vergés, J. C. Afonso, D. Garcia-Castellanos, and J. Fullea (2010), Lithospheric structure of the Gorringe Bank: Insights into its origin and tectonic evolution, *Tectonics*, *29*, TC5019, doi:10.1029/ 2009TC002458.

Jones, A. G. (1999), Imaging the continental upper mantle using electromagnetic methods, *Lithos*, *48*, 57–80.

Jones, A. G. (1998), Waves of future: Superior inferences from collocated seismic and electromagnetic experiments, *Tectonophysics*, *286*, 273–298.

Jones, A. G., and J. A. Craven (2004), Area selection for diamond exploration using deep-probing electromagnetic surveying, *Lithos*, *77* (1), 765–782.

Jones, A. G., Evans, R. L., and Eaton, D. W. (2009a), Velocity–conductivity relationships for mantle mineral asssemblages in Archean cratonic lithosphere based on a review of laboratory data and Hashin–Shtrikman extremal bounds, *Lithos*, *109*, 131–143.

Jones, A. G., et al. (2009b), Area selection for diamonds using magnetotellurics: Examples from southern Africa, *Lithos*, *112*, 83–92.

Jones, A. G., Plomerova, J., Korka, T., Sodoudi, F., and Spakman, W. (2010), Europe from the bottom up: A statistical examination of the central and northern European lithosphere–asthenosphere boundary from comparing seismological and electromagnetic observations, *Lithos*, *120*, 14–29.

Jones, A. G., Fullea, J., Evans, R. L., and Muller, M. R. (2012), Calibrating laboratory-determined models of electrical conductivity of mantle minerals using geophysical and petrological observations, *Geochem. Geophys. Geosyst. 13*, Q06010, doi:10.1029/2012GC004055.

Jordan, T. H. (1988), Structure and Formation of the Continental Tectosphere. *J. Petrol.*, *1*, 11–37.

Julia, J., C. J. Ammon, R. B. Herrmann, and A. M. Correig (2000), Joint inversion of receiver functions and surface-wave dispersion observations, *Geophys. J. Int.*, *143*, 99–112.

Julia, J., C. J. Ammon, and R. B. Herrmann (2003), Lithospheric structure of the Arabian Shield from the joint inversion of receiver functions and surface wave group velocities. *Tectonophysics*, *371*, 1–21.

Kaban, M. K., M. Tesauro, W. D. Mooney, and S. A. P. L. Cloetingh (2014), Density, temperature, and composition of the North American lithosphereNew insights from a joint analysis of seismic, gravity, and mineral physics data: 1. Density structure of the crust and upper mantle, *Geochem. Geophys. Geosyst.*,*15*,4781–4807,doi:10.1002/2014GC005483.

Karato, S.-I. (2011), Water distribution across the mantle transition zone and its implications for global material circulation, *Earth Planet. Sci. Lett.*, *301*, 413–423.

Karato, S.-I., and Wang, D. (2013), Electrical conductivity of minerals and rocks, in S.-I. Karato, ed., *Physics and Chemistry of the Deep Earth*, John Wiley & Sons, Hoboken, NJ, 145–182.

Karato, S-I. (1986), Does partial melting reduce the creep strengh of the upper mantle? *Nature*, *319*, 309–310.

Karato, S.-I. (2008), *Deformation of Earth materials: An Introduction to the Rheology of the Solid Earth*, Cambridge University Press, Cambridge, UK.

Karato, S. I., and H. Jung (1998), water, partial melting and the origin of the seismic low velocity and high attenuation zone in the upper mantle, *Earth Planet. Sci. Lett.*, *157*, 193–207.

Karato, S-I. (2012) On the origin of the asthenosphere, *Earth Planet. Sci. Lett.*, *321*, 95–103.

Kawakatsu, H., P. Kumar, Y. Takei, M. Shinohara, T. Kanazawa, E. Araki, and K. Suyehiro (2009), Seismic evidence for sharp lithosphere-asthenosphere boundaries of oceanic plates. *Science*, *324*, 499–502.

Kelbert, A., A. Schultz, and G. Egbert (2009), Global electromagnetic induction constraints on transition-zone water content variations, *Nature*, *460*, 1003–1006.

Kelemen, P.B, Hart, S.T., and S. Bernstein (1998), Silica enrichment in the continental upper mantle via melt/rock reaction, *Earth Planet. Sci. Lett.*, *164*, 387–406.

Khan, A., L. Boschi, and J. A. D. Connolly (2009), On mantle chemical and thermal heterogeneities and anisotropy as mapped by inversion of global surface wave data, *J. Geophys. Res.*, *114*, B09305, doi:10.1029/2009JB006399.

Khan, A., L. Boschi, and J. A. D. Connolly (2011), Mapping the Earth's thermochemical and anisotropic structure using global surface wave data, *J. Geophys. Res.*, *116*, B01301, doi:10.1029/2010JB007828.

Khan, A., and Shankland, T. J. (2012), A geophysical perspective on mantle water content and melting: inverting electromagnetic sounding data using laboratory-based electrical conductivity profiles, *Earth Planet. Sci. Lett.*, *317*, 27–43.

Khan, A., A. Zunino, and F. Deschamps (2013), Mantle thermochemical and anisotropic variations imaged beneath Australia from Bayesian inversion of surface-wave phase velocities, *J. Geophys. Res. Solid Earth*, *118*, 5285–5306, doi:10.1002/jgrb.50304.

Khan, A., S. Koch, T. J. Shankland, A. Zunino, and J. A. D. Connolly (2015), Relationships between seismic wave-speed, density, and electrical conductivity beneath Australia from seismology, mineralogy, and laboratory-based conductivity profiles, in *The Earths Heterogeneous Mantle—A Geophysical, Geodynamical, and Geochemical Perspective*, A. Khan and F. Deschamps, eds., Springer, New York, pp. 145–171.

Kind, R., X. Yuan, and P. Kumar (2012), Seismic receiver functions and the lithosphere–asthenosphere boundary, *Tectonophysics*, *536–537*, 25–43.

Kinzler, R. J., and T. L. Grove (1992) Primary Magmas of Mid-Ocean Ridge Basalts 1. Experiments and Methods. *J. Geophys. Res*., *97*(B5), 68856906, doi:10.1029/91JB02840.

Kissling, E., W. L. Ellsworth, D. Eberhart-Phillips, and U. Kradolfer (1994), Initial reference models in local earthquake tomography, *J. Geophys. Res.*, *99*, 19635–19646.

Koch, S., and A. Kuvshinov (2013), Global 3-D EM inversion of Sq variations based on simultaneous source and conductivity determination: Concept validation and resolution studies, *Geophys. J. Int.*, ggt227.

Kohlstedt, D. L., B. Evans, and S. J. Mackwell (1995), Strength of the lithosphere: Constraints imposed by laboratory experiments, *J. Geophys. Res.*, *100*, 17587–17602.

Kohlstedt, D. L., and M. E. Zimmerman (1996), Rheology of partially molten mantle rocks, *Annu. Rev. Earth Planet. Sci. 24*, 41–62.

Koyama, T., Khan, A., and Kuvshinov, A. (2014), Three-dimensional electrical conductivity structure beneath Australia from inversion of geomagnetic observatory data: Evidence for lateral variations in transition-zone temperature, water content and melt, *Geophys. J. Int.*, *196*, 1330–1350.

Kovács, I., D. H. Green, A. Rosenthal, J. Hermann, H. St C. O'Neill, W. Hibberson, and O. Udvardi (2012), An experimental study of water in nominally anhydrous minerals in the upper mantle near the water-saturated solidus, *J. Petrol.*, egs044.

Kumar, N., H. Zeyen, and A. P. Singh (2014), 3D lithosphere density structure of southern Indian shield from joint inversion of gravity, geoid, and topography data, *J. Asian Earth Sci.*, *89*, 98–107.

Kuskov, O. L., V. A. Kronrod, and A. A. Prokofev (2011), Thermal structure and thickness of the lithospheric mantle underlying the Siberian Craton from the Kraton and Kimberlite superlong seismic profiles, *Izvestiya, Physics of the Solid Earth*, *47*, 155–175.

Kuskov, O. L., V. A. Kronrod, and N. I. Pavlenkova. (2014), Thermodynamic–geophysical modeling of the interior structure of the Siberian cratonic mantle along cross-cutting profiles kimberlite and meteorite, *J. Geol. Geosci.*, *3*(155), 2.

Kuvshinov, A., and Semenov, A. (2012), Global 3-D imaging of mantle electrical conductivity based on inversion of observatory C-responses—I. An approach and its verification, *Geophys. J. Int.*, *189*, 13351352, doi:10.1111/j.1365-246X.2011.05349.x

Lachenbruch, A. H., and P. Morgan (1990), Continental extension, magmatism, and elevation: Formal relations and rules of thumb, *Tectonophysics*, *174*, 3962.

Lawrence, J. F., and D. A. Wiens (2004), Combine receiver-function and surface wave phase-velocity inversion using a niching genetic algorithm: Application to Patagonia, *Bull. Seismol. Soc Am.*, *94*(3), 977–987.

Ledo, J. and Jones, A.G. (2005), Upper mantle temperature determined from combining mineral composition, electrical conductivity laboratory studies and magnetotelluric field observations: Application to the intermontane belt, Northern Canadian Cordillera, *Earth Planet. Sci. Lett.*, *236*, 258–268.

Le Pichon, X., J., Francheteau, and J. Bonnin (1973), *Plate Tectonics, Developments in Geotectonics*, No. 6, Elsevier, Amsterdam, p. 300.

Le Roux, V., J.-L. Bodinier, A. Tommasi, O. Alard, J.-M. Dautria, A. Vauchez, and A. J. V. Riches (2007) The Lherz spinel lherzolite: Refertilized rather than pristine mantle, *Earth and Planet. Sci. Lett.*, *259*, 599–612, doi:10.1016/j.epsl.2007.05.026.

Lebedev, S., and R. D. van der Hilst (2008), Global upper-mantle tomography with the automated multimode inversion of surface and S-wave forms. *Geophys. J. Int.*, *173*, 505–518.

Lebedev, S., B. Endrun, M. Bischoff, and T. Meier (2007), Layering of seismic anisotropy and the past and present deformation on the lithosphere and asthenosphere beneath Germany, XXIV General Assembly of the IUGG, Perugia, Italy.

Lee, C.-T. A. (2003), Compositional variation of density and seismic velocities in natural peridotites at stp conditions: Implications for seismic imaging of compositional heterogeneites in the upper mantle, *J. Geophys. Res.*, *108*, doi:10.1029/2003JB002,413.

Liu, Q., and Gu, Y. J. (2012), Seismic Imaging: From classical to adjoint tomography, *Tectonophysics*, 566–567, 31–66.

Mandolesi, E., and A. G. Jones (2014), Magnetotelluric inversion based on mutual information, *Geophys. J. Int.*, *199*, 242–252.

Marler, R. T., and J. S. Arora (2004) Survey of multi-objective optimization methods for engineering, *Struct. Multidisc. Optim.*, *26*, 369–395.

Masson, F., and Trampert, J. (1997), On ACH, or how reliable is regional teleseismic delay time tomography? *Phys. Earth. Planet. Int.*, *102*, 21–32.

Matsukage, K. M., Y. Nishihara, and S. I. Karato (2005), Seismological signature of chemical differentiation of Earth's upper mantle, *J. Geophys. Res.*, *110*, B12305, doi:10.1029/2004JB003.

McDonough, W. F., and Sun, S.-S. (1995), Composition of the Earth, *Chemical Geology*, *120*: 223–253. doi: 10.1016/0009-2541(94)00140-4

Meltzer, A. (2003), EarthScope: Opportunities and challenges for earth-science research and education, *The Leading Edge*, *22*, 268–271.

McGary, R. S., and R. L. Evans, P. E. Wannamaker, J. Elsenbeck, and S. Rondenay (2014) Pathway from subducting slab to surface for melt and fluids beneath Mount Rainier, *Nature*, *511*(7509), 338–340.

Mei, S., and D. L. Kohlstedt (2000a), Influence of water on plastic deformation of olivine aggregates. 1. Diffusion creep regime, *J. Geophys. Res.*, *105*, B9, 21457–21469.

Mei, S., and D. L. Kohlstedt (2000b), Influence of water on plastic deformation of olivine aggregates. 2. dislocation creep regime, *J. Geophys. Res.*, *105*, B9, 21471–21481.

Meqbel, N. M., Egbert, G. D., Wannamaker, P. E., A. Kelbert, and A. Schultz (2014). Deep electrical resistivity structure of the northwestern US derived from 3-D inversion of USArray magnetotelluric data. *Earth Planet. Sci. Lett.*, *402*, 290–304.

Mierdel, K., H. Keppler, J. R. Smyth, and F. Langenhorst (2007), Water solubility in aluminous orthopyroxene and the origin of Earth's asthenosphere, *Science*, *315*, 364–368.

Mosegaard, K. (1998), Resolution analysis of general inverse problems through inverse Monte Carlo sampling, *Inverse Problems*, *14*, 405–426.

Mosegaard, K., and A. Tarantola (1995), Monte Carlo sampling of solutions to inverse problems, *J. Geophys. Res.*, *100*(B7), 12431–12447.

Mosegaard, K., and M. Sambridge (2002), Monte Carlo analysis of inverse problems, *Inverse Problems 18*, R29–R54.

Moorkamp, M., A. G. Jones, and D. W. Eaton (2007), Joint inversion of teleseismic receiver functions and magnetotelluric data using a genetic algorithm: Are seismic velocities and

electrical conductivities compatible?, *Geophys. Res. Lett.*, *34*, L16311.

Moorkamp, M., and A. G. Jones, and S. Fishwick (2010), Joint inversion of receiver functions, surface wave dispersion and magnetotelluric data, *J. Geophys. Res.*, *115*, B04318.

Naif, S., K. Key, S. Constable, and R. L. Evans (2013), Melt-rich channel observed at the lithosphere–asthenosphere boundary, *Nature*, *495*, 356–359.

Nolet, G. (2008), *A Breviary of Seismic Tomography: Imaging the interior of the Earth and the Sun*, Cambridge University Press, Cambridge, UK.

Nolet, G., S. P. Grand, and B. L. N. Kennett (1994), Seismic heterogeneity in the upper mantle, *J. Geophys. Res.*, *99*, 23753–23766.

Novella, D., D. J. Frost, E. H. Hauri, H. Bureau, C. Raepsaet, and M. Roberge (2014), The distribution of H_2O between silicate melt and nominally anhydrous peridotite and the onset of hydrous melting in the deep upper mantle, Earth, *Planet. Sci. Lett.*, *400*, 1–13.

Obrebski, M., R. M. Allen, F. Pollitz, and S. H. Hung, S. H. (2011), Lithosphere–asthenosphere interaction beneath the western United States from the joint inversion of body-wave traveltimes and surface-wave phase velocities, *Geophys. J. Int*., *185* (2), 1003–1021.

Olugboji T. M., S. Karato, and J. Park (2013), Structures of the oceanic lithosphere-asthenosphere boundary: Mineral-physics modeling and seismological signatures, *Geochem. Geophys. Geosyst.*, *14*, 880901, doi:10.1002/ggge.20086.

O'Reilly, S. Y. and W. L. Griffin (2010), The continental lithosphere–asthenosphere boundary: Can we sample it? *Lithos*, *120*, pp. 1–13.

O'Reilly, S. Y., and W. L. Griffin (2013), Mantle metasomatism, in *Metasomatism and the Chemical Transformation of Rock*, Springer, New York, pp. 471–533.

Olsen, N. (1999), Induction studies with satellite data, *Surv. Geophys.*, *20*, 309–340.

Olsen, N., et al. (2013), The Swarm satellite constellation application and research facility (SCARF) and Swarm data products, *Earth, Planets and Space*, *64*, 1189–1200.

Pail R., S. Bruinsma, F. Migliaccio, C. Frste, H. Goiginger, W.-D. Schuh, E. Hck, M. Reguzzoni, J. M. Brockmann, O. Abrikosov, M. Veicherts, T. Fecher, R. Mayrhofer, I. Krasbutter, F. Sans, and C. C. Tscherning (2011), First GOCE gravity field models derived by three different approaches; *J. Geodesy*, *85*(11), 819–843.

Panet, I., G. Pajot-Métivier, M. Greff-Lefftz, L. Métivier, M. Diament, and M. Mandea (2014), Mapping the mass distribution of Earth's mantle using satellite-derived gravity gradients, *Nature Geosci.*, *7*, 131–135.

Parsons, B., and S. Daly (1983), The relationship between surface topography, gravity anomalies, and temperature structure of convection, *J. Geophys. Res.*, *88*(B2), 11291144, doi:10.1029/JB088iB02p01129.

Pasyanos, M. E., and Nyblade, A. A. (2007), A top to bottom lithospheric study of Africa and Arabia, *Tectonophysics*, *444*, 27–44.

Pasyanos, M. E., T. G. Masters, G. Laske, Z. Ma (2014), LITHO1.0: An updated crust and lithospheric model of the Earth, *J. Geophys. Res.*, *119*, 2153–2173.

Pearson, D. G., D. Canil, and S. B. Shirey (2003), Mantle samples included in volcanic rocks: Xenoliths and diamonds, in *The Mantle and Core*, R. W. Carlson, ed., Vol. *2*, *Treatise on Geochemistry*, H. D. Holland, and K. K Turkeian, eds., Elsevier-Pergamon, Oxford, UK.

Pedreira, D., J. C. Afonso, J. A. Pulgar, J. Gallastegui, A. Carballo, M. Fernàndez, and O. García-Moreno (2015), Geophysical-petrological modeling of the lithosphere beneath the Cantabrian Mountains and the North-Iberian margin: Geodynamic implications, *Lithos*, *230*, 46–68.

Piccardo, G. B. 2008, The Jurassic Ligurian Tethys, a fossil ultraslow-spreading ocean: The mantle perspective, in *Metasomatism in Oceanic and Continental Lithospheric Mantle*, M. Cottorti and M. Gregoire, eds., Geological Society, London, Special Publications, 293, p. 1133.

Pinto, L. G. R., M. B. de Padua, N. Ussami, I. Vitorello, A. L. Padilha, and C. Braitenberg (2010) Magnetotelluric deep soundings, gravity and geoid in the south Sao Francisco craton: Geophysical indicators of cratonic lithosphere rejuvenation and crustal underplating, *Earth Planet. Sci. Lett.*, *297* 423434.

Plomerova, J., D. Kouba, and V. Babuska (2002), Mapping the lithosphere–asthenosphere boundary through changes in surface-wave anisotropy, *Tectonophysics*, *358*, 175–185.

Püthe, C., and Kuvshinov, A. (2014), Mapping 3-D mantle electrical conductivity from space: A new 3-D inversion scheme based on analysis of matrix Q-responses, *Geophys. J. Int.*, *197*, 768–784.

Poe, B. T., C. Romano, F. Nestola, and J. R. Smyth (2010), Electrical conductivity anisotropy of dry and hydrous olivine at 8GPa, *Phys. Earth Planet. Int.*, *181*, 103–111.

Priestley, K. F., and D. P. McKenzie (2006), The thermal structure of the lithosphere from shear wave velocities, *Earth Planet. Sci. Lett.*, *244*, 285–301.

Priestley, K., and F. Tilmann (2009), Relationship between the upper mantle high velocity seismic lid and the continental lithosphere, *Lithos*, *109*, 112124, doi:10.1016/j.lithos.2008.10.021.

Ranalli, G., *Rheology of the Earth*, 2nd ed., Chapman & Hall, London, 1995.

Rawlinson, N., S. Pozgay, and S. Fishwick (2010), Seismic tomography: A window into deep Earth, *Phys. Earth Planet. Int.*, *178*, 101–135.

Rawlinson, N., A. M. Reading, and B. L. N. Kennett (2006), Lithospheric structure of Tasmania from a novel form of teleseismic tomography, *J. Geophys. Res.*, *111*, B02301, doi:10.1029/2005JB003803.

Rawlinson, N., and S. Fishwick (2011), Seismic structure of the southeast Australian lithosphere from surface and body wave tomography, *Tectonophysics*, *572–573*, 111–122.

Rawlinson, N., and B. L. N. Kennett (2008), Teleseismic tomography of the upper mantle beneath the southern Lachlan Orogen, *Phys. Earth Planet. Int. 167*, 84–97

Rawlinson, N., A. Fichtner, M. Sambridge, and M. Young (2014), Seismic tomography and the assessment of uncertainty. *Adv. Geophys.*, *55*, 1–76, 10.1016/bs.agph.2014.08.001

Reguzzoni, M., Sampietro, D., Sansò, F. (2013), Global Moho from the combination of the CRUST2.0 model and GOCE data, *Geophys. J. Int*., ggt247.

Ricard, Y., L., Fleitout, and C. Froidevaux (1984), Geoid heights and lithospheric stresses for a dynamic Earth, *Ann. Geophys.*, *2*, 267–286.

Richards, M. A., and B. H. Hager (1989), Effects of lateral viscosity variations on long-wavelength geoid anomalies and

topography. *Journal of Geophysical Research 94*: doi: 10.1029/89JB00718. issn: 0148–0227.

Ritsema, J., W. Xu, L. Stixrude, and Lithgow-Bertelloni, C. (2009), Estimates of the transition zone temperature in a mechanically mixed upper mantle, *Earth Planet. Sci. Lett.*, *277*, 244–252, doi:10.1016/j.epsl.2008.10.024

Romanowicz, B. (2003), Global mantle tomography: progress status in the past 10 years, *Annu. Rev. Earth Planet. Sci.*, *31*, 303–328.

Roux, E., M. Moorkamp, A. G. Jones, and M. Bischoff, B. Endrun, S. Lebedev, and T. Meier (2011), Joint inversion of long-period magnetotelluric data and surface-wave dispersion curves for anisotropic structure: Application to data from Central Germany, *Geophys. Res. Lett.*, *38*(5), L05304.

Roy, M., J. K. MacCarthy, and J. Selverstone (2005), Upper mantle structure beneath the eastern Colorado Plateau and Rio Grande rift revealed by Bouguer gravity, seismic velocities, and xenolith data, Geochem. *Geophys., Geosys.*, *6*(10), doi:10.1029/2005GC001008.

Rychert, C. A., and P. M. Shearer (2011), Imaging the lithosphere–asthenosphere boundary beneath the Pacific using SS waveform modelling, *J. Geophys. Res.*, *116*, doi: 10.1029/2010JB008070

Sabaka, T. J., Olsen, N., and Purucker, M. E. (2004), Extending comprehensive models of the Earth's magnetic field with Ørsted and CHAMP data, *Geophys. J. Int.*, *159*, 521–547.

Sambridge, M. (1999), Geophysical inversion with a neighbourhood algorithm I. Searching a parameter space, *Geophys. J. Int.*, *138*, 479494.

Sandwell, D. T., and MacKenzie, K. R. (1989), Geoid height versus topography for oceanic plateaus and swells, *J. Geophys. Res. 94*: doi:10.1029/88JB03764. issn: 0148–0227.

Schaeffer, A. J., and S. Lebedev (2013), Global shear speed structure of the upper mantle and transition zone, *Geophys. J. Int.*, ggt095.

Schultz, A., R. D. Kurtz, A. D. Chave, and Jones, A. G. (1993), Conductivity discontinuities in the upper mantle beneath a stable craton, *Geophys. Res. Lett.*, *20*(24), 2941–2944.

Schulze, D. J. (1989), Constraints on the abundance of eclogite in the upper mantle, *J. Geophys. Res.*, *94*, 4205–4212.

Schutt, D. L., and Lesher, C.E. (2006) Effects of melt depletion on the density and seismic velocity of garnet and spinel lherzolite, *J. Geophys. Res.*, *111*, B05401, doi:10.1029/2003JB002.

Sclater, J. G., and J. Francheteau (1970), Implications of terrestrial heat flow observations on current tectonic and geochemical models of crust and upper mantle of earth, *Geophys. J. R. Astron. Soc. 20*, 509–542, 10.1111/j. 1365-246X.1970.tb06089.x

Semenov, A., and A. Kuvshinov (2012), Global 3-D imaging of mantle conductivity based on inversion of observatory C-responses—II. Data analysis and results, *Geophys. J. Int.*, *191*(3), 965–992.

Shan, B., J. C. Afonso, Y. Yang, C. J. Grose, Y. Zheng, X. Xiong, and L. Zhou (2014), The thermochemical structure of the lithosphere and upper mantle beneath south China: Results from multiobservable probabilistic inversion, *J. Geophys. Res. Solid Earth*, *119*, 84178441, doi:10.1002/2014JB011412.

Shen, W., M. H. Ritzwoller, and V. Schulte-Pelkum (2013), A 3-D model of the crust and uppermost mantle beneath the central and western US by joint inversion of receiver functions and surface wave dispersion, *J. Geophys. Res.*, doi:10.1029/2012JB009602.

Simpson, F., and A. Tommasi (2005), Hydrogen diffusivity and electrical anisotropy of a peridotite mantle, *Geophys. J. Int.*, *160*, 1092–1102.

Simmons, N. A., Forte, A. M., & Grand, S. P. (2006), Constraining mantle flow with seismic and geodynamic data: a joint approach. *Earth and Planetary Science Letters*, *246*(1), 109–124.

Simmons, N. A., A. M. Forte, L. Boschi, and S.P. Grand (2010), GyPSuM: A joint tomographic model of mantle density and seismic wave speeds, *J. Geophys. Res.*, *115*(12), B12310.

Shimizu, H., Koyama, T., Baba, K., and Utada, H. (2010), Revised 1-D mantle electrical conductivity structure beneath the north Pacific, *Geophys. J. Int.*, *180*, 1030–1048.

Speziale, S., F. Jiang, and T. S. Duffy (2005), Compositional dependence of the elastic wave velocities of mantle minerals: Implications for seismic properties of mantle rocks. Earth's deep mantle: structure, composition, and evolution, in *Geophys. Monograph*, Vol. *160*, ed., AGU, pp. 301–320.

Snyder, D. B., S. Rondenay, M. G. Bostock, and G. D. Lockhart (2004), Mapping the mantle lithosphere for diamond potential using teleseismic methods, *Lithos*, *77*, 859–872.

Stixrude, L., and C. Lithgow-Bertelloni (2011), Thermodynamics of mantle minerals II. Phase equilibria, *Geophys. J. Int.*, *184*, 11801213, doi:10.1111/j.1365-246X.2010.04890.x.

Stixrude, L., and C. Lithgow-Bertelloni (2005), Thermodynamics of mantle minerals: 1. Physical properties, *Geophys. J. Int.*, *162*, 610–632, 2005, doi: 10.1111/j.1365-246X.2005.02642.x

Stracke, A, and B. Bourdon (2009), The importance of melt extraction for tracing mantle heterogeneity, *Geochim. Cosmochim. Acta*, *73*, 218238.

Streckeisen, A. (1979), Classification and nomenclature of volcanic rocks, lamprophyres, carbonatites, and melilitic rocks: Recommendations and suggestions of the IUGS Subcommission on the Systematics of Igneous Rocks, *Geology*, *7* (7), 331–335.

Stolz, N. (2013), Bigger, better, smarter: high performance computers applied to Government geophysics, *ASEG Extended Abstracts 2013*(1), 1–4.

Tang, Y. J., H. F. Zhang, and J. F. Ying (2006), Asthenosphere lithospheric mantle interaction in an extensional regime: Implication from the geochemistry of Cenozoic basalts from Taihang Mountains, North China Craton, *Chem. Geol. 233*, 309327.

Tang, Y.-J., H.-F. Zhang, J.-F. Ying, and B.-X. Su (2007), Widespread refertilization of cratonic and circum-cratonic lithospheric mantle, *Earth Sci. Rev.*, *118*, 45–68.

Tarantola, A. (2005), *Inverse Problem Theory and Model Parameter Estimation*, Society for Industrial and Applied Mathematics, Philadelphia.

Tasaka, M., T. Hiraga, and M. E. Zimmerman (2013), Influence of mineral fraction on the rheological properties of forsterite+enstatite during grain-size-sensitive creep: 2. Deformation experiments, *J. Geophys. Res. Solid Earth*, *118*, 39914012, doi:10.1002/jgrb.50284.

Tašárová, A., J. C. Afonso, M. Bielik, H. J. Götze, and J. Hók (2009), The lithospheric structure of the Western Carpathian–Pannonian Basin region based on the CELEBRATION 2000 seismic experiment and gravity modelling, *Tectonophysics*, *475*(3), 454–469.

Tesauro, M., M. K. Kaban, W. D. Mooney, and S. A. P. L. Cloetingh (2014), Density, temperature, and composition of the North American lithosphere. New insights from a joint analysis of seismic, gravity, and mineral physics data: 2. Thermal and compositional model of the upper mantle, *Geochem. Geophys. Geosyst*., *15*, 48084830, doi:10.1002/2014GC005484.

Thybo, H. (2006), The heterogeneous upper mantle low velocity zone, *Tectonophysics*, *416*, 53–79.

Tiberi, C., M. Diament, J. Dverchre, C. Petit-Mariani, V. Mikhailov, S. Tikhotsky, and U. Achauer (2003), Deep structure of the Baikal rift zone revealed by joint inversion of gravity and seismology, *J. Geophys. Res*., *108*, 2133, doi:10.1029/2002JB001880, B3.

Tarits, P., and Mandéa, M. (2010), The heterogeneous electrical conductivity structure of the lower mantle, *Phys. Earth Planet. Int.*, *183*, 115–125.

Tkalcic, H., M. Pasyanos, A. Rodgers, R. Gok, W. Walter, A. Al-Amri (2006), Multistep method in joint modelling of receiver functions and surface waves: Implication for lithospheric structure of the Arabian Peninsula, *J. Geophys. Res.*, *B11311*, doi:10.1029/2005JB004130.

Torne, M., M. Fernandez, M. C. Comas, J. I. Soto (2000), Lithospheric structure beneath the Alboran Basin: Results from 3D gravity modelling and tectonic relevance, *J. Geophys. Res.*, *105*, 3209–3228.

Turcotte, D. L., and G. Schubert (2014), *Geodynamics*, Cambridge University Press, Cambridge, UK.

Unsworth, M., and P. A. Bedrosian (2004), Electrical resistivity structure at the SAFOD site from magnetotelluric exploration, *Geophys. Res. Lett*., *31*, L12S05.

Van Decar, J. C., and R. S. Crosson (1990), Determination of teleseismic relative phase arrival times using multichannel cross-correlation and least-squares, *Bull. Seism. Soc. Am.*, *80*, 150–169.

van Heijst, H. J., and J. Woodhouse (1999), Global high-resolution phase velocity distributions of overtone and fundamental-mode surface waves determined by mode branch stripping. *Geophys. J. Int.*, *137*(3), 601–620.

Velmskỳ, J. (2013), Determination of three-dimensional distribution of electrical conductivity in the Earth's mantle from Swarm satellite data: Time domain approach, *Earth Planets Space*, *65*, 1239–1246.

Visser, K., J. Trampert, S. Lebedev, and B. L. N Kennett (2008), Probability of radial anisotropy in the deep mantle, *Earth and Planetary Science Letters*, *270*(3), 241–250.

Vozar, J., A. G. Jones, J. Fullea, M. R. Agius, S. Lebedev, F. Le Pape, and W. Wei (2014), Integrated geophysical–petrological modeling of lithosphere-asthenosphere boundary in central Tibet using electromagnetic and seismic data, *Geochem. Geophys. Geosyst*., *15*, 39653988, doi:10.1002/2014GC005365.

Walter, M. J. (2003), Melt extraction and compositional variability in the mantle lithosphere, in *Treatise on Geochemistry*, Vol *2*, *The Mantle and Core*, R. W. Carlson, H. D. Holland, and K. K. Turekian, eds., Elsevier, Amsterdam, pp. 363–394.

Watts, A. B. (2011), Isostasy, In Encyclopedia of solid earth geophysics, Springer Netherlands, pp. 647–662.

Watts, A. B. (2001), Isostasy and Flexure of the Lithosphere, Cambridge University Press.

Wei, W., et al. (2001), Detection of widespread fluids in the Tibetan crust by magnetotelluric studies, *Science*, *292*, 716–718.

West, M., W. Gao, and S. Grand (2004) A simple approach to the joint inversion of seismic body and surface waves applied to the southwest US. *Geophys. Res. Lett*., *31*, L15615, doi:10.1029/2004GL020373.

Xu, W., C. Lithgow-Bertelloni, L. Stixrude, and J. Ritsema (2008), The effect of bulk composition and temperature on mantle seismic structure, *Earth Planet. Sci. Lett.*, *275*, 70–79, doi:10.1016/j.epsl.2008.08.012.

Xu, Y., T. J. Shankland, and B. T. Poe (2000), Laboratory-based electrical conductivity in the Earth's mantle, *J. Geophys. Res*., *105*, 27865–27875.

Yang, Y., and D. W. Forsyth (2006), Regional tomographic inversion of amplitude and phase of Rayleigh waves with 2-D sensitivity kernels, *Geophys. J. Int*., *166*, 1148–1160.

Yang, Y., M. H. Ritzwoller, F.-C. Lin, M. P. Moschetti, and N. M. Shapiro (2008), Structure of the crust and uppermost mantle beneath the western United States revealed by ambient noise and earthquake tomography, *J. Geophys. Res*., *113*, B12310, doi:10.1029/2008JB005833.

Yoshino, T., and T. Katsura (2013), Electrical conductivity of mantle minerals: Role of water in conductivity anomalies. *Annu. Rev. Earth Planet. Sci*., *41*, 601–628.

Yuan, H., R. Kind, X. Li, R. Wang (2006), The S receiver functios: Synthetics and data example. *Geophys. J. Int*., *165*, 555–564.

Yuan, H., S. French, P. Cupillard, and B. Romanowicz (2014), Lithospheric expression of geological units in central and eastern North America from full waveform tomography, *Earth Planet. Sci. Lett*., *402*, 176–186.

Zeyen, H., and M. Fernàndez (1994), Integrated lithospheric modeling combining thermal, gravity, and local isostasy analysis: Application to the NE Spanish Geotransect, *J. Geophys. Res*., *99*(B9), 18,08918,102, doi:10.1029/94JB00898.

Zeyen, H., and U. Achauer (1997), Joint inversion of teleseismic delay times and gravity anomaly data for regional structures: Theory and synthetic examples, in *Upper Mantle Heterogeneities from Active and Passive Seismology,* NATO Workshop, K. Fuchs, ed., Kluwer Academic Publishers, Norwell, MA, pp. 155–168.

Zeyen, H., P. Ayarza, M. Fernàndez, and A. Rimi (2005), Lithospheric structure under the western African-European plate boundary: A transect across the Atlas Mountains and the Gulf of Cadiz, *Tectonics*, *24*, TC2001, doi:10.1029/2004TC001639.

Zhang, H., and C. H. Thurber (2003), Double-difference tomography: The method and its application to the Hayward Fault, California, *Bull. Seis. Soc. Am*., *93*(5), 1875–1889, doi = 10.1785/0120020190.

Zhang, Y-S., and T. Tanimoto (1991), Global Love wave phase velocity variation and its significance to plate tectonics. *Phys. Earth Planet. Int*., *66*, 160–202.

Zhao, D., Yamamoto, Y., Yanada, T. (2013), Global mantle heterogeneity and its influence on teleseismic regional tomography, *Gondwana Res*., *23*, 595–616.

Zheng, Y., Lay, T., Flanagan, M. P., Williams, Q. (2007), Pervasive seismic reflectivity and metasomatism of the Tonga mantle wedge, *Science*, *316*, 855–859.